ENERGY EIGENVALUE AND THERMODYNAMIC PROPERTIES OF DENG-FAN SCREENING POTENTIAL WITH AB-FIELD

A Dissertation

Submitted to the Department of Physics,

Amrit Science Campus, Tribhuvan University, Leknath Marg, Lainchaur, in the Partial Fulfilment for the Requirement of Master's Degree in Physics

By

Ramkripal Sharma

Symbol No: 3591/076

Registration No: 5-2-50-450-2014

August, 2024

RECOMMENDATION

It is my pleasure to recommend Mr. *Ramkripal Sharma* has carried out the dissertation entitle **"Energy Eigenvalue and Thermodynamic Properties of Deng-Fan Screening Potential with AB-Field"** under our supervision. We recommend this dissertation submitted in partial fulfillment for the requirement of master degree of science in physics at Tribhuvan University.

…….	……..…….
Supervisor	Co-Supervisor
Assoc. Prof. Kishori Yadav, Ph.D.	Mr. Saddam Husain Dhobi, Ph.D. Scholar
Department of Physics, Patan Multiple Campus, Patan Dhoka, Tribhuvan University Lalitpur, Nepal.	Central Department of Physics, Tribhuvan University, Kirtipur, Kathmandu, Nepal

Date: …….

ACKNOWLEDGMENT

I would like to express my deep gratitude to my advisors Associate Prof. Dr. Kishori Yadav, Department of Physics, Patan Multiple Campus, Tribhuvan University. In addition, I would also like to thanks my Advisor Mr. Saddam Husain Dhobi, Ph.D. scholar, Central Department of physics, Tribhuvan University, Kirtipur, Kathmandu, Nepal for their patient guidance, enthusiastic encouragement, and useful critiques of this research work. Furthermore, I express my gratitude to Assoc. Prof. Janak Ratna Malla, Ph.D. who oversees the Physics Department, Prof. Pitamber Shrestha, the Coordinator Assistant Professor, and the entire faculty of Amrit Science Campus. I would also like to thank for coordination for their advice and assistance in keeping my progress in my research schedule. My thanks are also extended to all my family members who directly and indirectly help in this research work by providing a peaceful environment. Finally, I wish to thank my parents for their support and encouragement throughout my study.

EVALUATION

The undersigned that we read, approved, and recommended for dissertation of Master's in Physics Amrit Campus, Lainchaur, Kathmandu, Tribhuvan University, for accepting the term paper entitled **"Energy Eigenvalue and Thermodynamic Properties of Deng-Fan Screening Potential with AB-Field",** by Mr. *Ramkripal Sharma*

……..

Supervisor
Assoc. Prof. Kishori Yadav, Ph.D.
Department of Physics, Patan Multiple Campus, Tribhuvan University
Patan Dhoka, Lalitpur, Nepal

……..

Co-Supervisor
Mr. Saddam Husain Dhobi, Ph.D. Scholar
Central Department of Physics, Tribhuvan University, Kirtipur, Kathmandu, Nepal

……

Co-Ordinator
Assoc. Prof. Pitamber Shrestha
Department of Physics, Amrit Campus,
Tribhuvan University, Leknath Marg,
Lainchaur, Kathmandu, Nepal

……

Head of Department
Assoc. Prof. Janak Ratna Malla, Ph.D.
Department of Physics, Amrit Campus,
Tribhuvan University, Leknath Marg,
Lainchaur, Kathmandu, Nepal

……

Internal
Assistant Prof. Yogesh Maharjan
Department of Physics, Amrit Campus,
Tribhuvan University, Leknath Marg,
Lainchaur, Kathmandu, Nepal

……..……..

External
Assoc. Prof. Bal Ram Ghimire
Central Department of Physics, Tribhuvan University, Kirtipur, Kathmandu, Nepal

Date:……

ABSTRACT

This thesis investigates the quantum mechanical behavior of electrons in systems subjected to Deng-Fan screening potentials and AB-fields, with a focus on diatomic molecules (H_2, Cl_2, HCl). By employing the Schrödinger Wave Equation, the analysis integrates centrifugal and Greene-Aldrich approximations to explore electron dynamics. The study formulates an effective potential that incorporates the Deng-Fan potential, external magnetic fields, and other relevant terms, expressed through a dimensionless variable to facilitate numerical analysis. The investigation reveals that screening parameters consistently reduce repulsive potentials, with H2 exhibiting the highest potential energy. Energy eigenvalues decrease with increasing quantum numbers and magnetic flux, while higher screening parameters lead to more tightly bound electrons, particularly in the n=1 state. Additionally, magnetic fields are shown to reduce partition functions, with Cl_2 being more affected than H_2. These findings highlight the significant impact of screening and magnetic effects on molecular stability, providing valuable insights into quantum state-dependent electron behavior. This research contributes to the broader understanding of molecular interactions in quantum chemistry and molecular physics, with implications for condensed matter physics and quantum information science.

Keywords: Deng-Fan Screening Potential, AB-Field, Schrödinger Wave Equation, Centrifugal and Greene-Aldrich Approximations

शोधसार

यस थीसिसले डायटोमिक अणुहरू (H_2, Cl_2, HCl) मा फोकसको साथ, Deng-Fan स्क्रीनिंग क्षमता र AB-फिल्डहरूको अधीनमा रहेका प्रणालीहरूमा इलेक्ट्रोनहरूको क्वान्टम मेकानिकल व्यवहारको अनुसन्धान गर्दछ। Schrödinger Wave समीकरण प्रयोग गरेर, विश्लेषणले इलेक्ट्रोन गतिशीलता अन्वेषण गर्न केन्द्रापसारक र ग्रीन-एल्ड्रिच अनुमानहरू एकीकृत गर्दछ। अध्ययनले एक प्रभावकारी सम्भाव्यता बनाउँछ जसले डेंग-फ्यान सम्भाव्यता, बाह्य चुम्बकीय क्षेत्रहरू, र अन्य सान्दर्भिक सर्तहरू समावेश गर्दछ, संख्यात्मक विश्लेषणको सुविधाको लागि आयामरहित चर मार्फत व्यक्त गरिएको छ। अनुसन्धानले खुलासा गर्छ कि स्क्रीनिंग प्यारामिटरहरूले लगातार विकर्षक क्षमताहरू घटाउँछन्, H_2 ले उच्चतम सम्भावित ऊर्जा प्रदर्शन गर्दछ। बढ्दो क्वान्टम संख्या र चुम्बकीय प्रवाह संग ऊर्जा eigenvalues घट्छ, जबकि उच्च स्क्रीनिंग प्यारामिटरहरु लाई अधिक कडा बाउन्ड इलेक्ट्रोन को नेतृत्व गर्दछ, विशेष गरी n=1 स्थिति मा। थप रूपमा, चुम्बकीय क्षेत्रहरू विभाजन प्रकार्यहरू कम गर्न देखाइएको छ, Cl_2 H_2 भन्दा बढी प्रभावित भएको छ। यी खोजहरूले आणविक स्थिरतामा स्क्रीनिंग र चुम्बकीय प्रभावहरूको महत्त्वपूर्ण प्रभावलाई हाइलाइट गर्दछ, क्वान्टम राज्य-निर्भर इलेक्ट्रोन व्यवहारमा बहुमूल्य अन्तर्दृष्टि प्रदान गर्दछ। यस अनुसन्धानले क्वान्टम केमिस्ट्री र आणविक भौतिकीमा आणविक अन्तरक्रियाहरूको फराकिलो समझमा योगदान पुऱ्याउँछ, कन्डेन्ड पदार्थ भौतिकी र क्वान्टम सूचना विज्ञानको लागि प्रभावहरू सहित।

Table of Contents

LIST OF FIGURES

List of abbreviation

AB	Aharonov-Bohm
MR	Manning-Rosen
G	Gibbs free energy
H	enthalpy
S	entropy
GMP	Generalized Morse potential
B	magnetic field
A	Vector potential
SI	Shape invariance
AIM	asymptotic iteration method
NU	Nikiforov-Uvarov
FAA	functional analysis approach
SUSY	Supersymmetric

List of symbols

σ	screening constant
Z_{eff}	effective nuclear charge
V	potential
H_2	hydrogen molecues
Cl_2	chlorine
HCl	hydrochloric acid
n	quantum number
η	screening parameters
TiH	Titanium hydride

CHAPTER 1: INTRODUCTION

1.1 AB Field

A quantum phenomenon known as the Aharonov-Bohm (AB) effect casts doubt on traditional theories of electromagnetic. The AB effect, first proposed by David Bohm and Yakir Aharonov in 1959, shows that even in areas where the magnetic field (B) is zero, the vector potential (A) connected to the magnetic field known as AB field can have a detectable impact on quantum particles. Particles that go through an area with a non-zero vector potential, like electrons, develop a change in phase in their quantum wavefunction that produces noticeable interference effects. The AB effect shows that electromagnetic potentials are entirely quantum-mechanical and non-local, even in without the presence of a magnetic field in the area. To emphasize the effect's topological character, the phase change is quantized in terms of the elementary flux quantum. The AB effect's significance in comprehending the complex interaction between quantum mechanics as well as electromagnetic potentials is highlighted by experimental validations of the phenomenon, such as electron interfering experiments (Batelaan & Tonomura, 2009).

1.2 Screening parameters

Screening parameters are essential in explaining the intricate interactions between electrons inside an atom in atomic physics. These parameters, which are mainly defined by the screening constant (σ) and the effective nuclear charge (Zeff), capture the shielding action that inner electrons have on outer electrons. After accounting for the screening effect, the net positive charge that an electron experiences is represented by the effective nuclear charge. Because electrons have a negative charge, the screening effect lessens the electrostatic repulsion between them, which lowers the effective nuclear charge of the outer electrons. Within the atom, this phenomena has significant ramifications. Specifically, it affects electron-electron repulsion and produces a more stable arrangement of electrons. Furthermore, because outside electrons are less drawn to the nucleus, the screening effect aids in the enlargement of atomic size. Furthermore, it is essential in establishing electron affinity and ionization energy, which influence how simple it is to add or remove electrons from an atom. All things considered, a sophisticated comprehension of screening variables is essential for clarifying atomic characteristics, forecasting reactivity, and dissecting the complex dynamics controlling electrons within atoms (Safronova et al., 2018).

1.3 Thermodynamic properties

An easy and effective way to forecast the shift in the thermodynamics functions for a particular chemical reaction is to explicitly represent the thermodynamic characteristics of gaseous components. Though having a universal analytical expression to determine these properties for various molecules continues to be a formidable goal in physical as well as chemical engineering, understanding thermodynamic characteristics such as the enthalpy (H), entropy (S), as well as Gibbs free energy (G) for the chemical species in question is always the core purpose in both the practical and theoretical aspects of material processing. More research is currently being done on diatomic systems for a variety of uses in diverse domains, including phase transitions, adsorption, dissolution, and different chemical processes. In tandem with the latest developments in technology, scientists have been working on numerous theoretical methods to calculate thermodynamic functions and improve agreement with experimental data. Building a practical strategy for forecasting the course of events of thermodynamic variables requires a thorough understanding of intermolecular interactions. Numerous contributions, including as the Morse, Poschl-Teller, RosenMorse, Manning-Rosen, Tietz, Frost-Musulin, Schioberg, as well as Zavitsas functions, have gone into designing the oscillator potential models. The enhanced oscillator functions have drawn a great deal of interest while examining a range of the molecular spectroscopy parameters for explicit parameters and handling thermodynamic quantities of various diatomic substances. Calculating the vibrational part of the molecular partition function and, consequently, the associated thermodynamic parameters can be done with an appropriate oscillator function. For simulating intermolecular interactions and computing the thermodynamic parameters of diatomic molecules, several enhanced empirically potential models are useful in this regard. A major effort to compute certain thermodynamic quantities associated with diatomic molecules has been reported recently by Jia and colleagues. In this study, we aimed to propose a simplified method for examining the thermodynamic features of the HCl production reaction by taking the newly created Manning-Rosen (DMR) oscillator into account as the interatomic vibrational interaction throughout a broad temperature range. One of the elements of several chemical reactions with significant industrial and scientific implications is hydrogen chloride. The heat of formation of almost all metallic chlorides and many other compounds is calculated using the heat of formation of HCl. To do such an action, we must make use of the following relationship (Hesam et al., 2021):

$$\frac{1}{2}H_2(g) + \frac{1}{2}Cl_2(g) \rightarrow HCl(g) \quad (1)$$

where one mole of the intended material in its standard state is always formed by the reaction. We used just three molecular spectroscopic constants for each part of the reaction to achieve this goal. The generated results were compared with readily accessible experimental data at high temperatures as well as other theoretical approaches (Hesam et al., 2021).

1.4 Partition function

A partition function in physics characterizes the statistical characteristics of a thermodynamically balanced system. The thermodynamics state parameters, such as volume and temperature, are functions of partitions. A large number of the system's aggregate thermodynamic variables, including pressure, entropy, total energy, and free energy, can be represented in the form of the partition function or the derivatives of it. There is no dimension in the division function.Every partition function is designed to embody a specific statistical ensemble (which subsequently aligns with a specific free energy). Named partition functions are present in the majority of statistical ensembles. In a canonical ensemble, where the system is permitted to exchange heat with the surroundings at a set temperature, volume, and particle count, the canonical partition function is applicable. In a large canonical ensemble, where the system can exchange heat as well as particles with the environment at a given temperature, volume, as well as chemical potential, the grand canonical partition function is applicable. An exponential function representing the total of all conceivable energy for a system is all that is needed to determine its partition function. It is expected that each given state's many energies can be distinguished from one another. The partition function z was defined (Edet et al., 2022) as,

$$Z = \sum g_i e^{-\beta \epsilon_i} \; with \; \beta = \frac{1}{k_B T} \quad (2)$$

1.5 Generalized Morse potential

Analytical depictions of physical forces operating on a particle inside a predetermined region of space are known as potential functions or models. It has been applied to numerous physical process simulations. This is due to the fact that, in comparison to experimental and sophisticated computational approaches, it offers a comparatively less expensive method for modeling pertinent physical systems. Numerous potential functions have been used to model interatomic interactions in diatomic molecular systems. Depending on the type of interaction occurring within the system,

these possible functions change. The harmonic oscillator, the Morse potential, and a number of additional potentials that have been suggested are examples of such models. Recently, there have also been proposals for improving these models with additional fitting parameters in order to examine other physical systems. The idea that possible models with many fitting parameters tend to agree having experimental data more closely than those with a smaller number of parameters has motivated these developments, according to molecular physicists. This implies that there will always be a quest for fresh possible uses to suggest. The Deng-Fan potential, which is described as follows, is one of the many potentials that have been studied investigated and suggested as an enhancement to the potential previously mentioned; Wang et al. (2012) provided the developed Manning-Rosen (DMR) potential energy value for a diatomic oscillator as an additional relation by taking into account the Manning-Rosen function for the vibration potential energy. Described by Deng and Fan, the Generalized Morse potential (GMP) is associated with the Manning-Rosen potential (Hassanabadi et al., 2013),

$$V(r) = D_e \left[1 - \frac{b}{e^{\eta r} - 1}\right]^2 \tag{3}$$

where r_e is the equilibrium bond length, $b = e^{\eta r_e} - 1; 0 \leq r < \infty,$, D_e is the dissociation energy, $\eta$is the screening parameters that define the well's breadth, and r is the internuclear distance. Observe that its definition spans the same range as the real inter-nuclear potential in diatomic molecules, and that it exhibits the same behavior for $r \rightarrow 0$. A few shortcomings of the Morse potential have been noted in recent spectroscopic research. These shortcomings inspired Deng and Fan to develop a brand-new, enhanced potential known as the Deng-Fan, or generalized Morse potential. The potential was proposed in an effort to identify a more appropriate diatomic molecular potential to characterize the vibrational spectrum. It is a simple modification of the Morse potential.

It shares qualitative similarities with the Morse potential, but when the internuclear distance becomes closer to zero, it behaves correctly asymptotically. Using the Deng-Fan potential, several research in relativistic and non-relativistic quantum mechanics have been conducted. Given the foregoing, we are ready to investigate the effects of perturbations (magnetic and Aharonov-Bohm (AB) felds) on the thermal and magnetic characteristics of the Deng-Fan potential-modeled titanium hydroxide diatomic molecule. Titanium hydride (TiH) was chosen for this investigation because to its exceptional "hydrogen bonding" capability. Furthermore, metal hydrides are

commonly utilized in several industrial contexts, with one of its most notable uses being the storage of hydrogen. Although this hydride has undergone extensive theoretical and spectroscopic study, nothing is known about its thermo-magnetic characteristics. Given the molecule's tremendous interest and wide range of industrial applications, further research is required to fully understand its transport as well as thermo-magnetic properties—especially at higher temperatures—as well as other crucial aspects, as there is currently a dearth of information in the literature. Using the Hulthen-Kratzer potential (HKP) model, Edet and Ikot investigated the N_2, I_2, CO, NO, and HCl diatomic molecules in magnetic and AB fields. In light of the aforementioned, this study aims to assess, in line with earlier research, the effects of affecting external fields on the thermodynamic as well as magnetic characteristics of the Deng-Fan potential (Edet et al., 2022).

1.6 Different Method to Calculate Energy Eigen Value

1.6.1 Asymptotic iteration method

Second-order differential equations that are homogeneous linear and defined (Karki et al., 2022) as,

$$y''=\lambda_0(x)y'+s_0(x)y, \text{ here}\lambda_0(x) \text{ and}+s_0(x) \text{ function in}c_\infty(a,b) \tag{4}$$

By considering the derivatives of $(\mathrm{n}+1)^{th}$ and $(\mathrm{n}+2)^{th}$, we obtain

$$y^{(\mathrm{n}+1)}=\lambda_{\mathrm{n}-1}(x)y'+s_{\mathrm{n}-1}(x)y \text{ and } y^{\mathrm{n}+2}=\lambda_n(x)y'+s_n(x)y \tag{5}$$

Here $\lambda_n = \lambda'_{n-1}+s_{n-1}+\lambda_0\lambda_{n-1}$ and $s_n = s'_{n-1} + s_0\lambda_{n-1}$. Once the asymptotic condition is applied, the ratio of $(\mathrm{n}+2)^{th}$ and $(\mathrm{n}+1)^{th}$ is obtained. The condition $\frac{s_n}{\lambda_n} = \frac{s_{n-1}}{\lambda_{n-1}}$ yields the Eigenvalue of the equation under consideration, from which we derive $y^{n+1}(x) = c_1\lambda_{n-1}e^{\int(a+\lambda_0)dt}$. This formula produces the asymptotic consider equation's solution as

$$y(x) = \left[c_2 + c_1\int e^{\int(\lambda_0(\tau)+2\alpha(\tau)d\tau)dt}\right] \tag{6}$$

1.6.2 Nikiforov-Uvarov method

This technique is applied to solve an equation (such as the Schrodinger equation) by transformation (Oyewumi et al., 2013) as,

$$\psi''(s) + \frac{\tilde{\tau}(s)}{\sigma(s)} + \psi'(s)\frac{\tilde{\sigma}(s)}{\sigma^2(s)}\psi(s) = 0 \tag{7}$$

In this case, $\tilde{\sigma}(s)$ and $\dot{\tau}(s)$are second-degree polynomials, and $\dot{\tau}(s)$is a polynomial of degree at most one. Upon applying the $\lambda=\lambda_n$ one condition, the energy Eigenvalue can be obtained. Here,

the polynomials $\lambda=k\_+(s)$ and $\lambda n = -n\tau'(s)-\frac{n(n-s)\sigma''(s)}{2}$, $\pi(s)$ have four values that may be found by comparing the standard equation.

1.6.3 Super symmetry method

This approach assumes a specific sort of wave function in order to calculate the energy eigenvalue (Falaye et al., 2014).

$$\psi_s = exp[\int w_0(r)dr + \beta(r)]\phi_s(r) \tag{8}$$

In quantum mechanics, $w_0(r)$ represents super symmetry and is supposed to be the Witten super potential. A new function, $\phi_s(r)$, and a wave function, $\beta(r)$, also lead to the proper asymptotic value. Since we are aware, the Schrodinger equation may be used to find the energy eigenvalue for any potential by substituting ψ for the general wavefunction and solving the problem in a manner akin to the standard approach.

1.6.4 Factorization method

This method uses a factorization technique known as the separation of variables in general to separate the angular and radial part of the wave function for a given coordinate system (for example, the Schrodinger equation spherical coordinate system),

$$\Psi(r,\theta,\phi) = (r)\Theta(\theta)\Phi(\phi) \tag{9}$$

After separating the angular and radial parts.

1.6.5 Gauss Hyper Geometric

The Hypergeometric function is defined for $|z| < 1$ by (Karki et al., 2022) the power series

$$_2F_1(a,b;c;z) = \sum_{n=0}^{\infty} \frac{(a)_n(b)_n}{(c)_n}\frac{z^n}{n!} = 1 + \frac{ab}{c}\frac{z}{1!} + \frac{a(a+1)b(b+1)}{c(c+1)}\frac{z^2}{2!} + \cdots \tag{10}$$

The Poch hammer symbol in this case is represented by $(q)_n$= {1 for n=0 and q(q+1)….For n>0,... (q+n-1) Additionally, Euler's Hypergeometric Differential Equation is solved by the Hypergeometric function,

$$z(z-1)\frac{d^2\omega}{dz^2} + [c-(a+b+1))]\frac{d\omega}{dz} - ab\omega = 0 \tag{11}$$

This has 0,1, ∞, and three normal solitary points. Riemann's differential equation provides a generalization of the above equation to 3 arbitrary regular singular points. By switching variables, any second order linear differential problem with three periodic singular points can be transformed into a hypergeometric differential equation.

1.7 Objective

1.7.1 General objective

The objective of this thesis is to study the energy eigenvalue of screening Deng-fan potential with AB field.

1.7.2 Specific Objectives

- To develop theoretical model of energy eigenvalue for screening Deng-fan potential with AB field.
- To study nature of energy eigenvalue of H_2, Cl_2 and HCl with screening parameters in AB filed and its thermodynamic properties

CHAPTER 2: LITERATURE REVIEW

2.1 Related Review

The conventional method precisely presents the bound state solution of the s-wave radially Schrödinger equation with Manning-Rosen potential. It is discovered that the generalised hypergeometric functions ${}^2F_1(a, b; c; z)$ can be used to represent the solutions. We derive the unsolvable normalized wavefunctions. Additionally, we examine the unique scenario where $\alpha = 0$ and discover that this potential will decrease to the Hulthén potential; nonetheless, they do not employ a screening impact among the molecules (Dong and Ravelo, 2007).

Working on a complete square integrable basis carrying a tridiagonal matrix description of the wave operator allows one to study the Schrödinger equation with the Manning-Rosen potential. In this program, the expansion parameters of the wavefunction are found by solving the three-term recursion relation that results from solving the Schrödinger equation. By diagonalizing the recursion relation with specific parameter selection, the discrete spectra of the bound states is achieved, and the wavefunctions are described in terms of the Jocobi polynomial. The appropriate property of a diatomic molecule was proposed to be described by the Manning-Rosen potential. This potential has been the focus of numerous studies and is included in the exact solvable class. In the current work, we work in a complete squares integrable basis carrying a tridiagonal matrix description for the wave operator in an effort to study the Schrödinger equation with Manning-Rosen potential. By diagonalizing the recursion relationship with certain parameters, the discrete spectra of the bound states is derived, and the wavefunctions are described with the help of the Jocobi polynomial (Zhang & An, 2010).

A suitable approximate to the centrifugal term performs the nearly analytical bound state solutions to the l-wave Schrodinger problem for the ¨ Manning-Rosen MR potential. Applying the Nikiforov-Uvarov NU technique to the Manning-Rosen potential yields the energy spectrum formula as well as normalized wave functions defined in terms of the Jacobi polynomials. We compute the eigenvalues numerically for random principal as well as orbital quantum numbers n as well as l with two distinct values of the potential screening variable α in order to demonstrate the precision of our findings. Our results are shown to be in good agreement with the other methods' results for the lowest possible values of orbital quantum number l, α, and short potential

range. Investigated are two unique situations of great interest, such as the Hulthen potential case and the S-wave case (Ikhdair, 2012).

We achieved analytical approaches to the ℓ-wave solution of the Schrödinger equation based on the Manning-Rosen potential by using the asymptotic iteration method (AIM). Explicitly obtained are the energy eigenvalues formula and the accompanying wavefunctions. Regarding the centrifugal term, three distinct Pekeris-type approximation approaches have been applied. We have computed the eigenvalues computationally for arbitrary quantum numbers such as n and ℓ for a few diatomic molecules (HCl, CH, LiH, and CO) to demonstrate the precision of our findings. It is discovered that the outcomes agree well with other outcomes reported in the literature. Additionally, a simple extension to the Hulthén potential example and the s-wave case are given. Numerous academics have examined an approximate analytical solution for the Schrödinger equation with Manning-Rosen potential. Several areas of physics have leveraged this possibility for confined states and scattering features. The asymptotic iteration method was utilized to determine the approximate solution of the effective mass of this potential in N dimensions, and the Dirac equation containing this potential has also been examined. The spin–pseudospin symmetries associated with the Dirac equation with the real and general Manning–Rosen potentials were recently obtained by Hassanabadi et al. using the SUSY technique (Falayeet al., 2013).

The literature has recently published studies on the thermodynamic properties of several diatomic compounds using the improved Manning-Rosen potential model. Using the enhanced Manning-Rosen potential energy model's rotation-vibrational energy expression, Jia et al. investigated the thermodynamic characteristics of a lithium dimer. Using the enhanced Rosen-Morse potential energy model's rotation-vibrational energy expression, Song et al. additionally looked into the sodium dimer's thermodynamic features. Using the revised Manning-Rosenpotential, Wang et al. examined the entropy of gas boron monobromide and projected a four-parameter equation for determining the molar entropy without the need for extensive experimental spectroscopic data. Using the modified Rosen-Morsepotential, Deng and Jia investigated the molar enthalpy for nitrogen gas and projected a four-parameter expression for molar enthalpy calculation that does not require the use of extensive experimental spectroscopic data. Jia et al. investigated a four-parameter entropy expression for diatomic molecules, such as HCl, CO, BBr, HF, and DF, by employing the Tietz potential for internal vibration. Additionally, Peng et al. investigated the enhanced Rosen-Morse potential and developed an analytical model to forecast the gaseous

diatomic molecules' molar Gibbs free energies. Based on the enhanced Rosen-Morse oscillator potential to characterize a molecule's internal vibration, Jia et al. also looked into the molar enthalpy for gaseous compounds (Louisa et al., 2019).

An precise analytical equation for regular and irregular solutions in all partial waves of motion in the Manning-Rosen potential is constructed by utilizing the ordinary differential technique in conjunction with specific features of Gaussian hypergeometric functions. For a few lower partial waves, the Jost function derived from the irregular solution's near-origin behavior is suitably employed to calculate scattering phase variations for the neutron-proton as well as neutron-deuteron systems. Although we did not employ the screening effect, our results are in good accord with the experimental data (Khirali et al., 2020).

The parametric Nikiforov Uvarov technique is used to solve the Schrodinger equation using superposition of Manning-Rosen + inversely Mobius square + quadratic Yukawa potentials, together with an estimate of the centrifugal term. For every angular momentum quantum number l, the bound state energy eigenvalues and related un-normalized wave functions are computed. The mixed potential, coupled with their bound state energies, provides solutions for several potentials, including the Manning-Rosen, Mobius square, inversely quadratic Yukawa, and Hulthén potentials in specific instances. In quantum mechanics, different approaches have been devised and used recently to solve the equations for waves with a specific solvable potential. We list a few of the numerous approaches: shape invariance (SI), precise quantization rule, asymptotic iteration method (AIM), Nikiforov-Uvarov (NU) method, group theoretical technique, factorization method, functional analysis approach (FAA), and supersymmetric (SUSY) quantum mechanics. In recent years, there has been extensive consideration and study of the Manning-Rosen, quadratic Yukawa, and Mobius square potentials in both relativistic and non-relativistic wave equations. Thus, the primary goal of this work is to provide an approximate solution for the non-relativistic Schrödinger equation using the superposition of Yukawa potential models, Manning-Rosen models, and inversely Mobius square models. Therefore, in order to enable a mathematical solution of the equation of Schrödinger for any angle momentum quantum number l, we must consider the centrifugal factor using the Greene-Aldrich approximation. By using the parametric Nikiforov-Uvarov (pNU) approach, we could obtain the bound state energy spectrum and related wave functions for any angle momentum quantum number l (Faroutet al., 2021).

2.2 Research gap

Though there are still a number of unanswered questions, research on the Manning-Rosen potential as well as its applications has advanced significantly (Hassanabadi et al., 2013 and (Khirali et al., 2020)). First, taking into account the screening effect between the molecules and the AB field, it is necessary to investigate the thermodynamic characteristics of diatomic molecules with the Manning-Rosen potential. This would improve molecular behavior accuracy and comprehension. Second, further research needs to be done on the application of Gaussian hypergeometric functions to the construction of exact analytical approaches for the Manning-Rosen potential. This method may be applied to a wider variety of physical systems. Furthermore, a comparison of several approximation methods, like the asymptotic iteration method and the Nikiforov-Uvarov method, can highlight their advantages and disadvantages in certain situations. Our knowledge of the Manning-Rosen potential and its applications in the study of quantum systems, especially diatomic molecules, will improve if these research gaps are filled.

2.3 Siginifcant of work

For various reasons, the research on Manning-Rosen potential screening with AB field as well as its applications is very important. First, by taking into account the screening effect among molecules, examining the thermodynamic characteristics of diatomic molecules through the screening Manning-Rosen potential using AB field can help develop precise predictive models and offer insightful information about molecular behavior. Second, investigating how to build analytical solutions using Gaussian hypergeometric functions presents a viable path toward improving our comprehension of the screening Manning-Rosen potential with AB field. We can possibly examine a large class of physical systems other than diatomic molecules using this mathematical technique, which will improve our capacity to model and understand intricate quantum systems. Furthermore, researchers can determine the most appropriate approaches for various scenarios by performing a comparison of approximate techniques used in addressing the screening Manning-Rosen potential the formula with AB field. This enhances the accuracy and dependability of quantum mechanical calculations. Last but not least, for the screening Manning-Rosen potential model that includes AB field to be accurate and applicable, empirical confirmation of the theoretical predictions is essential.

2.4 Motivation of the research work

The motivation for this research stems from the intricate quantum mechanical behavior of electrons in diatomic molecules when subjected to complex potentials and external fields, specifically the Deng-Fan screening potential and AB-fields. Understanding these interactions is crucial for advancing our knowledge in quantum chemistry and molecular physics, as these factors significantly influence molecular stability and electron dynamics. The study's focus on diatomic molecules like H_2, Cl_2, and HCl, which are foundational in various chemical processes, further underscores the relevance of this research. By integrating centrifugal and Greene-Aldrich approximations with the Schrödinger Wave Equation, the research aims to provide deeper insights into the quantum state-dependent behavior of electrons. This work is particularly motivated by the need to elucidate how screening parameters and magnetic fields affect molecular interactions, which has broader implications for condensed matter physics and emerging fields like quantum information science.

CHAPTER 3: RESEARCH METHODOLOGY

3.1 Theoretical formulation

A radial variant of the Schrodinger Wave Equation (SE) is available (Edet and Ikot, 2021) as,

$$\psi''(r) + \frac{2m}{\hbar^2}\left[E_{nl} - V(r) - \frac{l(l+1)\hbar^2}{2mr^2}\right]\psi(r) = 0 \tag{12}$$

Greene and Aldrich approximation: using centrifugal approximation to eliminate centrifugal approximation (Faroutet al., 2021),

$$\frac{1}{r^2} = \frac{\eta^2}{(1-e^{-\eta r})^2} \tag{13}$$

Currently utilizing the possibility for Deng-fan screening provided (Hassanabadi et al., 2013) by

$$V(r) = D_e\left(1 - \frac{b}{e^{\eta r}-1}\right)^2 e^{-\eta r} \tag{14}$$

Now in presence of field equation (12) become

$$\left[\frac{1}{2\mu}\left(p + \frac{e}{c}A\right)^2 + V(r)\right]\psi(r,\phi) = E_{nl}\psi(r,\phi)$$

Where $A = \left(\frac{Be^{-\eta r}}{(1-e^{-\eta r})} + \frac{\phi_{AB}}{2\pi r}\right)$ and using operator for p and value of A above equation become

$$\left[\frac{1}{2\mu}\left((-i\hbar\nabla)^2 + (-i\hbar\nabla)\left\{\frac{e}{c}\left(\frac{Be^{-\eta r}}{(1-e^{-\eta r})} + \frac{\phi_{AB}}{2\pi r}\right)\right\} + \left\{\frac{e}{c}\left(\frac{Be^{-\eta r}}{(1-e^{-\eta r})} + \frac{\phi_{AB}}{2\pi r}\right)\right\}(-i\hbar\nabla) + \frac{e^2}{c^2}\left(\frac{Be^{-\eta r}}{(1-e^{-\eta r})} + \frac{\phi_{AB}}{2\pi r}\right)^2\right) + V(r)\right]\psi(r,\phi) = E_{nl}\psi(r,\phi)$$

On arranging we get,

$$\left[\frac{1}{2\mu}\left(-\hbar^2\nabla^2 + (-i\hbar\nabla)\left\{\frac{e}{c}\left(\frac{Br}{2} + \frac{\phi_{AB}}{2\pi r}\right)\hat{\phi}\right\} + \left\{\frac{e}{c}\left(\frac{Br}{2} + \frac{\phi_{AB}}{2\pi r}\right)\hat{\phi}\right\}(-i\hbar\nabla) + \frac{e^2}{c^2}\left(\frac{Br}{2} + \frac{\phi_{AB}}{2\pi r}\right)^2\right) + V(r)\right]\psi(r,\phi) = E_{nl}\psi(r,\phi)$$

Form this equation we have $\nabla^2\psi(r,\phi) = \frac{1}{\mathrm{r}}\frac{\partial}{\partial \mathrm{r}}\left(\mathrm{r}\frac{\partial}{\partial \mathrm{r}}\right)\psi(r,\phi) + \frac{1}{\mathrm{r}^2}\frac{\partial^2}{\partial \phi^2}\psi(r,\phi)$ and introducing new wave function $\psi(r,\phi) = \frac{R(r)e^{im\phi}}{\sqrt{r}}$ we have

$$\left[\frac{1}{r}\frac{\partial}{\partial r}\left(r\ \frac{\partial}{\partial r}\right) + \frac{1}{r^2}\frac{\partial^2}{\partial \phi^2}\right]\frac{R(r)e^{im\phi}}{\sqrt{r}} = \left[\frac{1}{r}\frac{\partial}{\partial r}\left(r\ \frac{\partial}{\partial r}\frac{R(r)e^{im\phi}}{\sqrt{r}}\right) + \frac{1}{r^2}\frac{\partial^2}{\partial \phi^2}\left(\frac{R(r)e^{im\phi}}{\sqrt{r}}\right)\right]$$

$$= \left[\frac{1}{r}\frac{\partial}{\partial r}\left(r\ \frac{\partial}{\partial r}\frac{R(r)e^{im\phi}}{\sqrt{r}}\right) - \frac{m^2}{r^2}\frac{R(r)e^{im\phi}}{\sqrt{r}}\right] = \left[\frac{d^2R}{dr^2} - \frac{m^2 - \frac{1}{4}}{r^2}\right]\frac{R(r)e^{im\phi}}{\sqrt{r}}$$

Simplifying the equation we have

$$\left[\frac{1}{2\mu}\left(-\hbar^2\nabla^2 + (-i\hbar\nabla)\left\{\frac{e}{c}\left(\frac{Be^{-\eta r}}{(1-e^{-\eta r})} + \frac{\phi_{AB}}{2\pi r}\right)\right\} + \left\{\frac{e}{c}\left(\frac{Be^{-\eta r}}{(1-e^{-\eta r})} + \frac{\phi_{AB}}{2\pi r}\right)\right\}(-i\hbar\nabla)\right.$$
$$\left. + \frac{e^2}{c^2}\left(\frac{Be^{-\eta r}}{(1-e^{-\eta r})} + \frac{\phi_{AB}}{2\pi r}\right)^2\right) + V(r)\Bigg]\psi(r,\phi) = E_{nl}\psi(r,\phi)$$

$$\left[\frac{-\hbar^2}{2\mu}\left(\nabla^2 + \frac{i}{\hbar}\nabla\left\{\frac{e}{c}\left(\frac{Be^{-\eta r}}{(1-e^{-\eta r})} + \frac{\phi_{AB}}{2\pi r}\right)\right\} + \frac{i}{\hbar}\left\{\frac{e}{c}\left(\frac{Be^{-\eta r}}{(1-e^{-\eta r})} + \frac{\phi_{AB}}{2\pi r}\right)\right\}\nabla\right.$$
$$\left. - \frac{e^2}{\hbar^2c^2}\left(\frac{Be^{-\eta r}}{(1-e^{-\eta r})} + \frac{\phi_{AB}}{2\pi r}\right)^2\right) + V(r)\Bigg]\psi(r,\phi) = E_{nl}\psi(r,\phi)$$

On arranging the equation we have,

$$\left[\left(\nabla^2 + \frac{i}{\hbar}\nabla\left\{\frac{e}{c}\left(\frac{Be^{-\eta r}}{(1-e^{-\eta r})} + \frac{\phi_{AB}}{2\pi r}\right)\right\} + \frac{i}{\hbar}\left\{\frac{e}{c}\left(\frac{Be^{-\eta r}}{(1-e^{-\eta r})} + \frac{\phi_{AB}}{2\pi r}\right)\right\}\nabla\right.$$
$$\left. - \frac{e^2}{\hbar^2c^2}\left(\frac{Be^{-\eta r}}{(1-e^{-\eta r})} + \frac{\phi_{AB}}{2\pi r}\right)^2\right) - \frac{2\mu}{\hbar^2}V(r)\Bigg]\psi(r,\phi) = -\frac{2\mu}{\hbar^2}E_{nl}\psi(r,\phi)$$

Again taking all the parameters in left hand side we get and standard equation to obtained the solution,

$$\left[\left(\nabla^2 + \frac{i}{\hbar}\nabla\left\{\frac{e}{c}\left(\frac{Be^{-\eta r}}{(1-e^{-\eta r})} + \frac{\phi_{AB}}{2\pi r}\right)\right\} + \frac{i}{\hbar}\left\{\frac{e}{c}\left(\frac{Be^{-\eta r}}{(1-e^{-\eta r})} + \frac{\phi_{AB}}{2\pi r}\right)\right\}\nabla\right.$$
$$\left. - \frac{e^2}{\hbar^2c^2}\left(\frac{Be^{-\eta r}}{(1-e^{-\eta r})} + \frac{\phi_{AB}}{2\pi r}\right)^2\right) + \frac{2\mu}{\hbar^2}\{E_{nl} - V(r)\}\Bigg]\psi(r,\phi) = 0$$

From above we have radial part as $\nabla^2\psi(r,\phi) = \left[\frac{d^2R}{dr^2} - \frac{m^2-\frac{1}{4}}{r^2}\right]\frac{R(r)e^{im\phi}}{\sqrt{r}}$ and putting the value fo $\nabla^2\psi(r,\phi)$ in above equation we get,

$$\left[\left(\left\{\frac{d^2R}{dr^2} - \frac{m^2-\frac{1}{4}}{r^2}\right\}\frac{R(r)e^{im\phi}}{\sqrt{r}} + \frac{i}{\hbar}\nabla\left\{\frac{e}{c}\left(\frac{Be^{-\eta r}}{(1-e^{-\eta r})} + \frac{\phi_{AB}}{2\pi r}\right)\right\}\frac{R(r)e^{im\phi}}{\sqrt{r}}\right.$$
$$+ \frac{i}{\hbar}\left\{\frac{e}{c}\left(\frac{Be^{-\eta r}}{(1-e^{-\eta r})} + \frac{\phi_{AB}}{2\pi r}\right)\right\}\nabla\left(\frac{R(r)e^{im\phi}}{\sqrt{r}}\right)$$
$$\left. - \frac{e^2}{\hbar^2c^2}\left(\frac{Be^{-\eta r}}{(1-e^{-\eta r})} + \frac{\phi_{AB}}{2\pi r}\right)^2\frac{R(r)e^{im\phi}}{\sqrt{r}}\right) + \frac{2\mu}{\hbar^2}\{E_{nl} - V(r)\}\frac{R(r)e^{im\phi}}{\sqrt{r}}\Bigg] = 0$$

Solving and arranging we get,

$$\left[\left(\left\{\frac{d^2R}{dr^2} - \frac{m^2-\frac{1}{4}}{r^2}\right\}\frac{R(r)e^{im\phi}}{\sqrt{r}} + \frac{i}{\hbar}\nabla\left\{\frac{e}{c}\left(\frac{Be^{-\eta r}}{(1-e^{-\eta r})} + \frac{\phi_{AB}}{2\pi r}\right)\right\}\frac{R(r)e^{im\phi}}{\sqrt{r}}\right.$$
$$+ \frac{i}{\hbar}\left\{\frac{e}{c}\left(\frac{Be^{-\eta r}}{(1-e^{-\eta r})} + \frac{\phi_{AB}}{2\pi r}\right)\right\}\nabla\left(\frac{R(r)e^{im\phi}}{\sqrt{r}}\right)$$
$$\left. - \frac{e^2}{\hbar^2c^2}\left(\frac{Be^{-\eta r}}{(1-e^{-\eta r})} + \frac{\phi_{AB}}{2\pi r}\right)^2\frac{R(r)e^{im\phi}}{\sqrt{r}}\right) + \frac{2\mu}{\hbar^2}\{E_{nl} - V(r)\}\frac{R(r)e^{im\phi}}{\sqrt{r}}\Bigg] = 0$$

As we $A = \left(\frac{Be^{-\eta r}}{(1-e^{-\eta r})} + \frac{\phi_{AB}}{2\pi r}\right)^2 = \frac{B^2e^{2\eta r}}{(1-e^{\eta r})^2} + \frac{\phi_{AB}Be^{-\eta r}}{\pi r(1-e^{-\eta r})} + \frac{\phi_{AB}^2}{4\pi^2r^2}$ again expanding we get

$$\left[\left(\left\{\frac{d^2R}{dr^2}-\frac{m^2-\frac{1}{4}}{r^2}\right\}\frac{R(r)e^{im\phi}}{\sqrt{r}}+\frac{i}{\hbar}\nabla\left\{\frac{e}{c}\left(\frac{Be^{-\eta r}}{(1-e^{-\eta r})}+\frac{\phi_{AB}}{2\pi r}\right)\right\}\frac{R(r)e^{im\phi}}{\sqrt{r}}\right.\right.$$
$$+\frac{i}{\hbar}\left\{\frac{e}{c}\left(\frac{Be^{-\eta r}}{(1-e^{-\eta r})}+\frac{\phi_{AB}}{2\pi r}\right)\right\}\nabla\left(\frac{R(r)e^{im\phi}}{\sqrt{r}}\right)$$
$$\left.-\frac{e^2}{\hbar^2c^2}\left(\frac{B^2e^{2\eta r}}{(1-e^{\eta r})^2}+\frac{\phi_{AB}Be^{-\eta r}}{\pi r(1-e^{-\eta r})}+\frac{\phi_{AB}^2}{4\pi^2r^2}\right)\frac{R(r)e^{im\phi}}{\sqrt{r}}\right)$$
$$\left.+\frac{2\mu}{\hbar^2}\{E_{nl}-V(r)\}\frac{R(r)e^{im\phi}}{\sqrt{r}}\right]=0$$

Solving and arranging the equation for variables we get

$$\left[\left(\left\{\frac{d^2R}{dr^2}-\frac{m^2-\frac{1}{4}}{r^2}\right\}\frac{R(r)e^{im\phi}}{\sqrt{r}}+\frac{i}{\hbar}\nabla\left\{\frac{e}{c}\left(\frac{Be^{-\eta r}}{(1-e^{-\eta r})}+\frac{\phi_{AB}}{2\pi r}\right)\right\}\frac{R(r)e^{im\phi}}{\sqrt{r}}\right.\right.$$
$$+\frac{i}{\hbar}\left\{\frac{e}{c}\left(\frac{Be^{-\eta r}}{(1-e^{-\eta r})}+\frac{\phi_{AB}}{2\pi r}\right)\right\}\nabla\left(\frac{R(r)e^{im\phi}}{\sqrt{r}}\right)$$
$$\left.-\left(\frac{B^2e^{2\eta r}e^2}{\hbar^2c^2(1-e^{\eta r})^2}+\frac{\phi_{AB}Be^{-\eta r}e^2}{\hbar^2c^2\pi r(1-e^{-\eta r})}+\frac{\phi_{AB}^2e^2}{4\hbar^2c^2\pi^2r^2}\right)\frac{R(r)e^{im\phi}}{\sqrt{r}}\right)$$
$$\left.+\frac{2\mu}{\hbar^2}\{E_{nl}-V(r)\}\frac{R(r)e^{im\phi}}{\sqrt{r}}\right]=0$$

Finally arranging above equation we get

$$\left[\left(\left\{\frac{d^2R}{dr^2}-\frac{m^2-\frac{1}{4}}{r^2}\right\}\frac{R(r)e^{im\phi}}{\sqrt{r}}+\frac{i}{\hbar}\left\{\frac{e}{c}\left(\frac{Be^{-\eta r}}{(1-e^{-\eta r})}+\frac{\phi_{AB}}{2\pi r}\right)\right\}\frac{R(r)e^{im\phi}}{\sqrt{r}}\right.\right.$$
$$+\frac{i}{\hbar}\left\{\frac{e}{c}\left(\frac{Be^{-\eta r}}{(1-e^{-\eta r})}+\frac{\phi_{AB}}{2\pi r}\right)\right\}\nabla\left(\frac{R(r)e^{im\phi}}{\sqrt{r}}\right)$$
$$\left.-\left(\frac{B^2e^{2\eta r}e^2}{\hbar^2c^2(1-e^{\eta r})^2}+\frac{\phi_{AB}Be^{-\eta r}e^2}{\hbar^2c^2\pi r(1-e^{-\eta r})}+\frac{\phi_{AB}^2e^2}{4\hbar^2c^2\pi^2r^2}\right)\frac{R(r)e^{im\phi}}{\sqrt{r}}\right)$$
$$\left.+\frac{2\mu}{\hbar^2}\{E_{nl}-V(r)\}\frac{R(r)e^{im\phi}}{\sqrt{r}}\right]=0$$

On removing the imaginary term $\frac{i}{\hbar}\left\{\frac{e}{c}\left(\frac{B}{2}-\frac{\phi_{AB}}{4\pi r^2}\right)\hat{\phi}\right\}\frac{R(r)e^{im\phi}}{\sqrt{r}}$ and solving we get

$$\frac{i}{\hbar}\left\{\frac{e}{c}\left(\frac{\boldsymbol{Be^{-\eta r}}}{(\mathbf{1}-\boldsymbol{e^{-\eta r}})}+\frac{\boldsymbol{\phi_{AB}}}{\boldsymbol{2\pi r}}\right)\hat{\phi}\right\}\nabla\left(\frac{R(r)e^{im\phi}}{\sqrt{r}}\right)=-\frac{\mathrm{em}}{\hbar\mathrm{c}}\left(\frac{\boldsymbol{Be^{-\eta r}}}{(\mathbf{1}-\boldsymbol{e^{-\eta r}})}+\frac{\boldsymbol{\phi_{AB}}}{\boldsymbol{2\pi r}}\right)\frac{R(r)e^{im\phi}}{r^{\frac{3}{2}}}$$
$$=-\frac{\mathrm{em}}{\hbar\mathrm{c}}\left(\frac{\boldsymbol{Be^{-\eta r}}}{(\mathbf{1}-\boldsymbol{e^{-\eta r}})}+\frac{\boldsymbol{\phi_{AB}}}{\boldsymbol{2\pi r}}\right)\frac{R(r)e^{im\phi}}{r^{\frac{1}{2}}.r}-\left(\frac{emBe^{-\eta r}}{\hbar\mathrm{cr}(\mathbf{1}-\boldsymbol{e^{-\eta r}})}+\frac{em\phi_{AB}}{2\pi\hbar cr^2}\right)\frac{R(r)e^{im\phi}}{\sqrt{r}}$$

Putting the valese in above equation after removing the value we get

$$\left[\left(\left\{\frac{d^2R}{dr^2}-\frac{m^2-\frac{1}{4}}{r^2}\right\}\frac{R(r)e^{im\phi}}{\sqrt{r}}-\left(\frac{emBe^{-\eta r}}{\hbar\mathrm{cr}(1-e^{-\eta r})}+\frac{em\phi_{AB}}{2\pi\hbar cr^2}\right)\frac{R(r)e^{im\phi}}{\sqrt{r}}\right.\right.$$
$$\left.-\left(\frac{B^2e^{-2\eta r}e^2}{\hbar^2c^2(1-e^{-\eta r})^2}+\frac{\phi_{AB}Be^{-\eta r}e^2}{\hbar^2c^2\pi r(1-e^{-\eta r})}+\frac{\phi_{AB}^2e^2}{4\hbar^2c^2\pi^2r^2}\right)\frac{R(r)e^{im\phi}}{\sqrt{r}}\right)$$
$$\left.+\frac{2\mu}{\hbar^2}\{E_{nl}-V(r)\}\frac{R(r)e^{im\phi}}{\sqrt{r}}\right]=0$$

Now we have $\xi=\frac{\phi_{AB}}{\phi_0}$, $\phi_0=\frac{hc}{e}$, $\omega=\frac{eB}{\mu c}$

$$\left[\left(\left\{\frac{d^2R}{dr^2}-\frac{m^2-\frac{1}{4}}{r^2}\right\}\frac{R(r)e^{im\phi}}{\sqrt{r}}-\left(\frac{m\omega\hbar e^{-\eta r}}{\mathrm{r}(1-e^{-\eta r})}+\frac{em\phi_{AB}}{2\pi\hbar \mathrm{c}r^2}\right)\frac{R(r)e^{im\phi}}{\sqrt{r}}\right.\right.$$
$$\left.-\left(\frac{\mu^2\omega^2}{\hbar^2}\frac{e^{-2\eta r}}{(1-e^{\eta r})^2}+\frac{\xi\omega_c e^{-\eta r}}{r(1-e^{-\eta r})}+\frac{\phi_{AB}^2e^2}{4\hbar^2c^2\pi^2r^2}\right)\frac{R(r)e^{im\phi}}{\sqrt{r}}\right)$$
$$\left.+\frac{2\mu}{\hbar^2}\{E_{nl}-V(r)\}\frac{R(r)e^{im\phi}}{\sqrt{r}}\right]=0$$

Solving with different steps as below for solution

$$\left[\left(\left\{\frac{d^2R}{dr^2}-\frac{m^2-\frac{1}{4}}{r^2}\right\}\frac{R(r)e^{im\phi}}{\sqrt{r}}-\left(\hbar\omega_{\mathrm{c}}(\mathrm{m}+\xi)\frac{e^{-\eta r}}{\mathrm{r}(1-e^{-\eta r})}\right)\frac{R(r)e^{im\phi}}{\sqrt{r}}-\frac{em\phi_{AB}}{2\pi\hbar \mathrm{c}r^2}\frac{R(r)e^{im\phi}}{\sqrt{r}}\right.\right.$$
$$\left.\left.-\left(\frac{\mu^2\omega^2}{\hbar^2}\frac{e^{-2\eta r}}{(1-e^{\eta r})^2}+\frac{\phi_{AB}^2e^2}{4\hbar^2c^2\pi^2r^2}\right)\frac{R(r)e^{im\phi}}{\sqrt{r}}\right)+\frac{2\mu}{\hbar^2}\{E_{nl}-V(r)\}\frac{R(r)e^{im\phi}}{\sqrt{r}}\right]$$
$$=0$$

Simplifying the equation for solution we have

$$\left[\left(\left\{\frac{d^2R}{dr^2}-\frac{m^2-\frac{1}{4}}{r^2}\right\}\frac{R(r)e^{im\phi}}{\sqrt{r}}-\left(\hbar\omega_{\mathrm{c}}(\mathrm{m}+\xi)\frac{e^{-\eta r}}{\mathrm{r}(1-e^{-\eta r})}\right)\frac{R(r)e^{im\phi}}{\sqrt{r}}-\frac{em\phi_{AB}}{2\pi\hbar \mathrm{c}r^2}\frac{R(r)e^{im\phi}}{\sqrt{r}}\right.\right.$$
$$\left.-\left(\frac{\phi_{AB}^2e^2}{4\hbar^2c^2\pi^2r^2}\right)\frac{R(r)e^{im\phi}}{\sqrt{r}}\right)-\frac{\mu^2\omega^2}{\hbar^2}\frac{e^{-2\eta r}}{(1-e^{\eta r})^2}\frac{R(r)e^{im\phi}}{\sqrt{r}}$$
$$\left.+\frac{2\mu}{\hbar^2}\{E_{nl}-V(r)\}\frac{R(r)e^{im\phi}}{\sqrt{r}}\right]=0$$

$$\left[\left(\left\{\frac{d^2R}{dr^2}\right\}\frac{R(r)e^{im\phi}}{\sqrt{r}}-\left(\hbar\omega_c(\mathrm{m}+\xi)\frac{e^{-\eta r}}{\mathrm{r}(1-e^{-\eta r})}\right)\frac{R(r)e^{im\phi}}{\sqrt{r}}\right)-\frac{\mu^2\omega^2}{\hbar^2}\frac{e^{-2\eta r}}{(1-e^{\eta r})^2}\frac{R(r)e^{im\phi}}{\sqrt{r}}\right.$$
$$\left.-\left(\frac{m^2-\frac{1}{4}}{r^2}+\frac{em\phi_{AB}}{2\pi\hbar cr^2}+\frac{\phi_{AB}^2e^2}{4\hbar^2c^2\pi^2r^2}\right)\frac{R(r)e^{im\phi}}{\sqrt{r}}+\frac{2\mu}{\hbar^2}\{E_{nl}-V(r)\}\frac{R(r)e^{im\phi}}{\sqrt{r}}\right]$$
$$=0$$

$$\left[\left(\left\{\frac{d^2R}{dr^2}\right\}\frac{R(r)e^{im\phi}}{\sqrt{r}}-\left(\hbar\omega_c(\mathrm{m}+\xi)\frac{e^{-\eta r}}{\mathrm{r}(1-e^{-\eta r})}\right)\frac{R(r)e^{im\phi}}{\sqrt{r}}\right)-\frac{\mu^2\omega^2}{\hbar^2}\frac{e^{-2\eta r}}{(1-e^{\eta r})^2}\frac{R(r)e^{im\phi}}{\sqrt{r}}\right.$$
$$\left.-\left(\frac{m^2-\frac{1}{4}}{r^2}+\frac{em\phi_{AB}}{2\pi\hbar cr^2}+\frac{\phi_{AB}^2e^2}{4\hbar^2c^2\pi^2r^2}\right)\frac{R(r)e^{im\phi}}{\sqrt{r}}+\frac{2\mu}{\hbar^2}\{E_{nl}-V(r)\}\frac{R(r)e^{im\phi}}{\sqrt{r}}\right]$$
$$=0$$

Since we have $\xi=\frac{\phi_{AB}}{\phi_0}$, $\phi_0=\frac{hc}{e}$, $\omega=\frac{eB}{\mu c}$ and hence for $\frac{1}{r^2}\left(m^2-\frac{1}{4}+\frac{em\phi_{AB}}{2\pi\hbar cr^2}+\frac{\phi_{AB}^2e^2}{4\hbar^2c^2\pi^2r^2}\right)==$ $\frac{1}{r^2}\left(m^2+\frac{m\xi}{\pi}+\frac{\xi^2}{4\pi^2}-\frac{1}{4}\right)$. Therefore, the above equation become,

$$\left[\left(\left\{\frac{d^2R}{dr^2}\right\}\frac{R(r)e^{im\phi}}{\sqrt{r}}-\left(\hbar\omega_c(\mathrm{m}+\xi)\frac{e^{-\eta r}}{\mathrm{r}(1-e^{-\eta r})}\right)\frac{R(r)e^{im\phi}}{\sqrt{r}}\right)-\frac{\mu^2\omega^2}{\hbar^2}\frac{e^{-2\eta r}}{(1-e^{\eta r})^2}\frac{R(r)e^{im\phi}}{\sqrt{r}}\right.$$
$$-\frac{1}{r^2}\left\{\left(m+\frac{\xi}{2\pi}\right)^2-\frac{1}{4}\right\}\frac{R(r)e^{im\phi}}{\sqrt{r}}-\frac{e^2B^2r^2}{4\hbar^2c^2}\frac{R(r)e^{im\phi}}{\sqrt{r}}-\frac{emB}{2\hbar\mathrm{c}}\frac{R(r)e^{im\phi}}{\sqrt{r}}$$
$$\left.+\frac{2\mu}{\hbar^2}\{E_{nl}-V(r)\}\frac{R(r)e^{im\phi}}{\sqrt{r}}\right]=0$$

Arranging the parameters and variable we have

$$\left[\frac{d^2R}{dr^2}-\hbar\omega_c(\mathrm{m}+\xi)\frac{e^{-\eta r}}{\mathrm{r}(1-e^{-\eta r})}-\frac{\mu^2\omega^2}{\hbar^2}\frac{e^{-2\eta r}}{(1-e^{\eta r})^2}-\frac{1}{r^2}\left\{\left(m+\frac{\xi}{2\pi}\right)^2-\frac{1}{4}\right\}-\frac{e^2B^2r^2}{4\hbar^2c^2}-\frac{emB}{2\hbar\mathrm{c}}\right.$$
$$\left.+\frac{2\mu}{\hbar^2}\{E_{nl}-V(r)\}\right]=0$$

Bringing this equation in standard form as

$$\left[\frac{d^2R}{dr^2}+\frac{2\mu}{\hbar^2}\{E_{nl}-V(r)\}-\hbar\omega_c(m+\xi)\frac{e^{-\eta r}}{r(1-e^{-\eta r})}-\frac{\mu^2\omega^2}{\hbar^2}\frac{e^{-2\eta r}}{(1-e^{\eta r})^2}-\frac{1}{r^2}\left\{\left(m+\frac{\xi}{2\pi}\right)^2-\frac{1}{4}\right\}-\frac{e^2B^2r^2}{4\hbar^2c^2}-\frac{emB}{2\hbar c}\right]=0 \quad (15)$$

Let, $z=e^{-\eta r}$ and hence $z=\frac{1}{e^{\eta r}} => e^{\eta r}=\frac{1}{z}$, Now from equation (15) we have

$$\left[\frac{d^2R}{dr^2}+\frac{2\mu}{\hbar^2}\{E_{nl}-V(r)\}-\hbar\omega_c(m+\xi)\frac{z}{r(1-z)}-\frac{\mu^2\omega^2}{\hbar^2}\frac{z^2}{(1-z)^2}-\frac{1}{r^2}\left\{\left(m+\frac{\xi}{2\pi}\right)^2-\frac{1}{4}\right\}-\frac{e^2B^2r^2}{4\hbar^2c^2}-\frac{emB}{2\hbar c}\right]=0$$

Now effective potential is

$$V_{eff}(r)=D_e\left(1-\frac{b}{e^{\eta r}-1}\right)^2e^{-\eta r}+\hbar\omega_c(m+\xi)\frac{z}{r(1-z)}+\frac{\mu^2\omega^2}{\hbar^2}\frac{z^2}{(1-z)^2}+\frac{1}{r^2}\left\{\left(m+\frac{\xi}{2\pi}\right)^2-\frac{1}{4}\right\}+\frac{e^2B^2r^2}{4\hbar^2c^2}+\frac{emB}{2\hbar c}$$

Using centrifugal approximation of equation (13) $\frac{1}{r^2}=\frac{\eta^2}{(1-e^{-\eta r})^2}=\frac{\eta^2}{(1-z)^2}$ we get the readical part equation in ABfield

$$\left[\frac{d^2R}{dr^2}+\frac{2\mu}{\hbar^2}\{E_{nl}-V(r)\}-\hbar\omega_c(m+\xi)\frac{z\eta}{(1-z)^2}-\frac{\mu^2\omega^2}{\hbar^2}\frac{z^2}{(1-z)^2}-\frac{\eta^2}{(1-z)^2}\left\{\left(m+\frac{\xi}{2\pi}\right)^2-\frac{1}{4}\right\}-\frac{e^2B^2(1-z)^2}{4\hbar^2c^2\eta^2}-\frac{emB}{2\hbar c}\right]=0$$

Let as also simplify the assume potential as $V(r)=D_e\left(1-\frac{b}{e^{\eta r}-1}\right)^2e^{-\eta r}$, $z=e^{-\eta r} => e^{\eta r}=\frac{1}{z}$ then it become $V(r)=D_e\left(1-\frac{bz}{1-z}\right)^2z$ and hence radial equation become,

$$\left[\frac{d^2R}{dr^2}+\frac{2\mu}{\hbar^2}\left\{E_{nl}-D_e\left(1-\frac{bz}{1-z}\right)^2z\right\}-\hbar\omega_c(m+\xi)\frac{z\eta}{(1-z)^2}-\frac{\mu^2\omega^2}{\hbar^2}\frac{z^2}{(1-z)^2}-\frac{\eta^2}{(1-z)^2}\left\{\left(m+\frac{\xi}{2\pi}\right)^2-\frac{1}{4}\right\}-\frac{e^2B^2(1-z)^2}{4\hbar^2c^2\eta^2}-\frac{emB}{2\hbar c}\right]=0$$

No in term of radial wave function the radial equation can be expressed as,

$$\psi''(r)+\frac{2m}{\hbar^2}\left[E_{nl}-D_e\left(1-\frac{b}{\frac{1}{z}-1}\right)^2 z--\hbar\omega_c(\mathrm{m}+\xi)\frac{z\eta}{(1-z)^2}-\frac{\mu^2\omega^2}{\hbar^2}\frac{z^2}{(1-z)^2}\right.$$
$$\left.-\frac{\eta^2}{(1-z)^2}\left\{\left(m+\frac{\xi}{2\pi}\right)^2-\frac{1}{4}\right\}-\frac{e^2B^2(1-z)^2}{4\hbar^2c^2\eta^2}-\frac{emB}{2\hbar c}\right]\psi(r)=0$$

$$\psi''(r)+\frac{2m}{\hbar^2}\left[E_{nl}-D_e\left(1-\frac{b}{\frac{1-z}{z}}\right)^2 \mathrm{z}--\hbar\omega_c(\mathrm{m}+\xi)\frac{z\eta}{(1-z)^2}-\frac{\mu^2\omega^2}{\hbar^2}\frac{z^2}{(1-z)^2}\right.$$
$$\left.-\frac{\eta^2}{(1-z)^2}\left\{\left(m+\frac{\xi}{2\pi}\right)^2-\frac{1}{4}\right\}-\frac{e^2B^2(1-z)^2}{4\hbar^2c^2\eta^2}-\frac{emB}{2\hbar c}\right]\psi(r)=0$$

$$\psi''(r)+\frac{2m}{\hbar^2}\left[E_{nl}-D_e\left(1-\frac{bz}{1-z}\right)^2 \mathrm{z}-\hbar\omega_c(\mathrm{m}+\xi)\frac{z\eta}{(1-z)^2}-\frac{\mu^2\omega^2}{\hbar^2}\frac{z^2}{(1-z)^2}\right.$$
$$\left.-\frac{\eta^2}{(1-z)^2}\left\{\left(m+\frac{\xi}{2\pi}\right)^2-\frac{1}{4}\right\}-\frac{e^2B^2(1-z)^2}{4\hbar^2c^2\eta^2}-\frac{emB}{2\hbar c}\right]\psi(r)=0$$

$$\psi''(r)+\frac{2m}{\hbar^2}\left[E_{nl}-D_ez\left(1-\frac{2bz}{(1-z)}+\frac{b^2z^2}{(1-z)^2}\right)-\hbar\omega_c(\mathrm{m}+\xi)\frac{z\eta}{(1-z)^2}-\frac{\mu^2\omega^2}{\hbar^2}\frac{z^2}{(1-z)^2}\right.$$
$$\left.-\frac{\eta^2}{(1-z)^2}\left\{\left(m+\frac{\xi}{2\pi}\right)^2-\frac{1}{4}\right\}-\frac{e^2B^2(1-z)^2}{4\hbar^2c^2\eta^2}-\frac{emB}{2\hbar c}\right]\psi(r)=0\ (16)$$

Again,$\frac{\partial \mathrm{z}}{\partial \mathrm{r}}=\frac{\partial(\mathrm{e}^{-\eta \mathrm{r}})}{\partial \mathrm{r}}=-\eta e^{-\eta r}=-\eta z$

$$\frac{\partial^2 z}{\partial r^2}=\frac{\partial}{\partial \mathrm{r}}\left(\frac{\partial \mathrm{z}}{\partial \mathrm{r}}\right)=\frac{\partial}{\partial \mathrm{r}}(-\eta \mathrm{e}^{-\eta r})=-\eta\frac{\partial \mathrm{e}^{-\eta \mathrm{r}}}{\partial \mathrm{r}}=-\eta\frac{\partial \mathrm{z}}{\partial \mathrm{r}}=-\eta(-\eta e^{-\eta r})=\eta^2 e^{-\eta r}=\eta^2 z$$

Again,$\frac{\partial \psi(\mathrm{r})}{\partial \mathrm{r}}=\frac{\partial \psi(\mathrm{z})}{\partial \mathrm{z}}\frac{\partial \mathrm{z}}{\partial \mathrm{r}}=\frac{\partial \psi(\mathrm{z})}{\partial \mathrm{z}}(-\eta e^{-\eta r})=-\psi'(z)\eta e^{-\eta r}=-\eta\psi'(z)z$

$$\frac{\partial^2\psi(r)}{\partial \mathrm{r}^2}=\frac{\partial\left(\frac{\partial \psi(\mathrm{r})}{\partial \mathrm{r}}\right)}{\partial \mathrm{z}}\times\frac{\partial \mathrm{z}}{\partial \mathrm{r}}=\left[\frac{\partial\{-\psi'(\mathrm{z})\eta \mathrm{e}^{-\eta \mathrm{r}}\}}{\partial \mathrm{z}}\right](-\eta e^{-\eta r})=\left[\frac{-\eta\,\partial\{\psi'(\mathrm{z})\mathrm{z}\}}{\partial \mathrm{z}}\right](-\eta z)$$

$$\psi''(r) = \{\eta^2 z(\psi''(z)z + \psi'(z)\}$$

$$\psi''(r) = -\eta\{\psi"(z)z + \psi'(z)\}(-\eta z)$$

$$\psi''(r) = \eta^2 z\{\psi"(z)z + \psi'(z)\}$$

$$\psi''(r) = \eta^2 z^2\psi"(z) + \eta^2 z\psi'(z)$$

$$\psi''(r) = \eta^2 z^2\psi''(z) + \eta^2 z\psi'(z) \quad (17)$$

Substituting the value in equation (16), we get

$$\eta^2 z^2\psi''(z) + \eta^2 z\psi'(z) + \left[\frac{2\mu E_{nl}}{\hbar^2} - \frac{2\mu}{\hbar^2}D_e z + \frac{4D_e\mu b z^2}{\hbar^2(1-z)} - \frac{2\mu}{\hbar^2}\frac{b^2 z^3 D_e}{(1-z)^2} - \hbar\omega_c(m+\xi)\frac{z\eta}{(1-z)^2} - \frac{\mu^2\omega^2}{\hbar^2}\frac{z^2}{(1-z)^2} - \frac{\eta^2}{(1-z)^2}\left\{\left(m+\frac{\xi}{2\pi}\right)^2 - \frac{1}{4}\right\} - \frac{e^2B^2(1-z)^2}{4\hbar^2c^2\eta^2} - \frac{emB}{2\hbar c}\right]\psi(z) = 0$$

$$\psi''(z) + \frac{\psi'(z)}{z} + \left[\frac{2\mu E_{nl}}{\hbar^2\eta^2 z^2} - \frac{2\mu D_e}{\hbar^2\eta^2 z} + \frac{4\mu b D_e}{\hbar^2\eta^2 z(1-z)} - \frac{2\mu b^2 D_e z}{\hbar^2\eta^2(1-z)^2} - \hbar\omega_c(m+\xi)\frac{z\eta}{(1-z)^2} - \frac{\mu^2\omega^2}{\hbar^2}\frac{z^2}{(1-z)^2} - \frac{\eta^2}{(1-z)^2}\left\{\left(m+\frac{\xi}{2\pi}\right)^2 - \frac{1}{4}\right\} - \frac{e^2B^2(1-z)^2}{4\hbar^2c^2\eta^2} - \frac{emB}{2\hbar c}\right]\psi(z) = 0$$

Multiple by $z(z-1)$ on both side

$$\psi''(z)z(z-1) + \psi'(z)(z-1) + \left[\frac{2\mu E_{nl}(z-1)}{\hbar^2\eta^2 z} - \frac{2\mu D_e(z-1)}{\hbar^2\eta^2} - \frac{4\mu b D_e}{\hbar^2\eta^2 z} - \left\{\frac{2\mu b^2 D_e}{\hbar^2\eta^2} + \hbar\omega_c\eta(m+\xi)\right\}\frac{z^2}{(1-z)} - \frac{\mu^2\omega^2}{\hbar^2}\frac{\boldsymbol{z^3}}{(\boldsymbol{1-z})} - \frac{z\eta^2}{(1-z)}\left\{\left(m+\frac{\xi}{2\pi}\right)^2 - \frac{1}{4}\right\} - \frac{e^2B^2z(z-1)^3}{4\hbar^2c^2\eta^2} - \frac{emBz(z-1)}{2\hbar c}\right]\psi(z) \quad (18)$$

Let $\frac{2\mu E_{nl}}{\hbar^2\eta^2} = -\epsilon, \frac{2\mu D_e}{\hbar^2\eta^2} = \sigma, \frac{4\mu b D_e}{\hbar^2\eta^2} = \delta, \left\{\frac{2\mu b^2 D_e}{\hbar^2\eta^2} + \hbar\omega_c\eta(\mathrm{m}+\xi)\right\} = \alpha, \frac{\mu^2\omega^2}{\hbar^2} = \beta_1, \eta^2\left\{\left(m+\frac{\xi}{2\pi}\right)^2 - \frac{1}{4}\right\} = \beta_2, \frac{e^2B^2}{4\hbar^2c^2\eta^2} = \beta_3, \frac{emB}{2\hbar c} = \beta_4$ Now above equation become

$$\psi''(z)\mathrm{z}(\mathrm{z}-1) + \psi'(z)(z-1) + \left[\frac{-\epsilon(z-1)}{z} - \sigma(z-1) - \frac{\delta}{z} - \alpha\frac{z^2}{(1-z)} - \beta_1\frac{z^3}{(1-z)} - \frac{\beta_2 z}{(1-z)} - \beta_3 z(z-1)^3 - \beta_4 z(z-1)\right]\psi(\mathrm{z}) \quad (18)$$

Now asymptotic behavior of equation (14), at $r\to 0$(z→ 1) and r→ ∞(z→ 0 then equation (18)become

$$\psi''(z)\mathrm{z}(\mathrm{z}-1) + \psi'(z)(z-1) + \left[\frac{-\epsilon(z-1)}{z} - \sigma(z-1) - \frac{\delta}{z} - \frac{\alpha}{(1-z)} - \frac{\beta_1}{(1-z)} - \frac{\beta_2}{(1-z)} - \beta_3(z-1)^3 - \beta_4(z-1)\right]\psi(\mathrm{z})$$

$$\psi''(z)\mathrm{z}(\mathrm{z}-1) + \psi'(z)(z-1) + \left[\frac{-\epsilon(z-1)}{z} - (\sigma+\beta_4)(z-1) - \frac{\delta}{z} + \frac{1}{(z-1)}\{\alpha+\beta_1+\beta_2\} - \beta_3(z-1)^3\right]\psi(\mathrm{z}) \quad (19)$$

Let us introduce a new function $f(z)$ as

$$\psi(z) = z^{\mu}(1-z)^{\phi}f(z) \quad (20)$$

Taking first derivate of equation (20) we get,

$$\psi'(z) = \mu z^{\mu-1}(1-z)^{\phi}f(z) - z^{\mu}\phi(1-z)^{\phi-1}f(z) + z^{\mu}(1-z)^{\phi}f'(z) \quad (21)$$

Also taking second derivative equation (20) we get,

$$\psi''(z) = \mu(\mu-1)z^{\mu-2}(1-z)^{\phi}f(z) - \phi\mu z^{\mu-1}(1-z)^{\phi-1}f(z) + \mu z^{\mu-1}(1-z)^{\phi}f'(z) - \phi\mu z^{\mu-1}(1-z)^{\phi-1}f(z) + \phi z^{\mu}(\phi-1)(1-z)^{\phi-2}f(z) - \phi z^{\mu}(1-z)^{\phi-1}f'(z) + \mu z^{\mu-1}(1-z)^{\phi}f'(z) - z^{\mu}\phi(1-z)^{\phi-1}f'(z) + z^{\mu}(1-z)^{\phi}f''(z)$$

And arranging we get

$$\psi''(z) = z^{\mu}(1-z)^{\phi}f''(z) + 2\mu z^{\mu-1}(1-z)^{\phi}f'(z) - 2\phi z^{\mu}(1-z)^{\phi-1}f'(z) - 2\phi\mu z^{\mu-1}(1-z)^{\phi-1}f(z) + \phi z^{\mu}(\phi-1)(1-z)^{\phi-2}f(z) + \mu(\mu-1)z^{\mu-2}(1-z)^{\phi}f(z) \quad (22)$$

Now Substituting the value of $\psi''(z), \psi'(z)$ and $\psi(z)$ from above in equation (19) we get,

$$z^{\mu+1}(1-z)^{\phi+1}f''(z) + 2\mu z^{\mu}(1-z)^{\phi+1}f'(z) - 2\phi z^{\mu+1}(1-z)^{\phi}f'(z) - 2\mu\phi z^{\mu}(1-z)^{\phi}f(z) + \phi z^{\mu+1}(\phi-1)(1-z)^{\phi-1}f(z) + \mu(\mu-1)z^{\mu-1}(1-z)^{\phi+1}f(z) + \mu z^{\mu-1}(1-z)^{\phi+1}f(z) - z^{\mu}\phi(1-z)^{\phi}f(z) + z^{\mu}(1-z)^{\phi+1}f'(z) + \left[\frac{-\epsilon(z-1)}{z} - (\sigma+\beta_4)(z-1) - \frac{\delta}{z} + \frac{1}{(z-1)}\{\alpha+\beta_1+\beta_2\} - \beta_3(z-1)^3\right] z^{\mu}(1-z)^{\phi}f(z) = 0$$

Taking z^{μ} and $(1-z)^{\phi}$ comment we get,

$$\mathrm{z}(1-\mathrm{z})f''(z) + 2\mu(1-z)f'(z) - 2\phi z f'(z) + (1-z)f'(z) - 2\mu\phi f(z) + \frac{\phi(\phi-1)z}{(1-z)}f(z) + \frac{\mu(\mu-1)(1-z)}{z}f(z) + \frac{\mu(1-z)}{z}f(z) - \phi f(z) + \left[\frac{-\epsilon(z-1)}{z} - (\sigma+\beta_4)(z-1) - \frac{\delta}{z} + \frac{1}{(z-1)}\{\alpha+\beta_1+\beta_2\} - \beta_3(z-1)^3\right] f(z) = 0$$

Arrange for the coefficient$f"(z)$, $f'(z)$ and $f(z)$ we get

$$\mathrm{z}(1-\mathrm{z})f''(z) + [2\mu(1-z) - 2\phi z + (1-z)]f'(z) - \left[2\mu\phi - \frac{\phi(\phi-1)z}{(1-z)} - \frac{\mu(\mu-1)(1-z)}{z} - \frac{\mu(1-z)}{z} + \phi\right] f(z) + \left[\frac{-\epsilon(z-1)}{z} - (\sigma+\beta_4)(z-1) - \frac{\delta}{z} + \frac{1}{(z-1)}\{\alpha+\beta_1+\beta_2\} - \beta_3(z-1)^3\right] f(z) = 0$$

Simplification we get,

$$z(1-z)f''(z) + [2\mu - 2\mu z - 2\phi z + 1 - z]f'(z) - \left[2\mu\phi - \frac{\phi^2 z}{(1-z)} + \frac{\phi z}{(1-z)} - \frac{\mu^{2(}(1-z)}{z} + \frac{\mu(1-z)}{z} - \frac{\mu}{z} + \mu + \phi\right] f(z) + \left[\frac{-\epsilon(z-1)}{z} - (\sigma + \beta_4)(z-1) - \frac{\delta}{z} + \frac{1}{(z-1)}\{\alpha + \beta_1 + \beta_2\} - \beta_3(z-1)^3\right] f(z) = 0$$

For, more simplification we get,

$$z(1-z)f''(z) + [(1+2\mu) - (2\mu + 2\phi + 1)z]f'(z) - \left[2\mu\phi - \frac{\phi^2 z}{(1-z)} + \frac{\phi z}{(1-z)} - \frac{\mu^2}{z} + \mu^2 + \frac{\mu}{z} - \mu - \frac{\mu}{z} + \mu + \phi\right] f(z) + \left[\frac{-\epsilon(z-1)}{z} - (\sigma + \beta_4)(z-1) - \frac{\delta}{z} + \frac{1}{(z-1)}\{\alpha + \beta_1 + \beta_2\} - \beta_3(z-1)^3\right] f(z) = 0$$

Multiplication of minus sign in second last term,

Or, $z(1-z)f''(z) + [(1+2\mu) - (2\mu + 2\phi + 1)z]f'(z) + \left[-2\mu\phi + \frac{\phi^2 z}{(1-z)} - \frac{\phi z}{(1-z)} + \frac{\mu^2}{z} - \mu^2 - \phi\right] f(z) + \left[\frac{-\epsilon(z-1)}{z} - (\sigma + \beta_4)(z-1) - \frac{\delta}{z} + \frac{1}{(z-1)}\{\alpha + \beta_1 + \beta_2\} - \beta_3(z-1)^3\right] f(z) = 0$

Arranging two last terms like below

$$\frac{\phi^2 z}{(1-z)} - \frac{\phi^2}{(1-z)} = \frac{\phi^2 z - \phi^2}{(1-z)} = \frac{\phi^2(z-1)}{(1-z)} = -\frac{\phi^2(1-z)}{(1-z)} = -\phi^2 => \frac{\phi^2 z}{(1-z)} = -\phi^2 + \frac{\phi^2}{(1-z)}$$

Using this relation in above equation we get,

$$z(1-z)f''(z) + [(1+2\mu) - (2\mu + 2\phi + 1)z]f'(z) + [-\phi^2 - 2\mu\phi - \mu^2 - \phi - \mu]f(z) + \left[\frac{-\epsilon(z-1)}{z} - (\sigma + \beta_4)(z-1) - \frac{\delta}{z} + \frac{1}{(z-1)}\{\alpha + \beta_1 + \beta_2\} - \beta_3(z-1)^3 + \frac{\phi^2}{(1-z)} + \frac{\mu^2}{z} - \frac{\phi z}{(1-z)}\right] f(z) = 0$$

Simplification of this equation we get

$$\mathrm{z}(1-\mathrm{z})f''(z)+[(1+2\mu)-(2\mu+2\phi+1)z]f'(z)+[-(\mu^2+2\mu\phi+\phi^2)-(\mu+\phi)]f(z)$$
$$+\left[\frac{-\epsilon(z-1)}{z}-(\sigma+\beta_4)(z-1)-\frac{\delta}{z}+\frac{1}{(z-1)}\{\alpha+\beta_1+\beta_2\}-\beta_3(z-1)^3\right.$$
$$\left.+\frac{\phi^2}{(1-z)}+\frac{\mu^2}{z}-\frac{\phi z}{(1-z)}+\mu\right]f(z)=0$$

$$\mathrm{z}(1-\mathrm{z})f''(z)-[(1+2\mu)-(2\mu+2\phi+1)z]f'(z)-[(\mu+\phi)^2+(\mu+\phi)]f(z)$$
$$+\left[\frac{-\epsilon(z-1)}{z}-(\sigma+\beta_4)(z-1)-\frac{\delta}{z}+\frac{1}{(z-1)}\{\alpha+\beta_1+\beta_2\}-\beta_3(z-1)^3\right.$$
$$\left.+\frac{\phi^2}{(1-z)}+\frac{\mu^2}{z}-\frac{\phi z}{(1-z)}+\mu\right]f(z)=0$$

Arranging the variable and constant we get

$$\mathrm{z}(1-\mathrm{z})f''(z)+[(1+2\mu)-(2\mu+2\phi+1)z]f'(z)-[(\mu+\phi)^2+(\mu+\phi)]f(z)$$
$$+\left[\frac{-\epsilon}{z}+\epsilon-(\sigma z\ -\ \sigma\ +\ \beta^4 z\ -\ \beta^4)-\frac{\delta}{z}+\frac{1}{(z-1)}\{\alpha+\beta_1+\beta_2\}\right.$$
$$\left.-\beta_3(z^3-3z^2+3z-1)+\frac{\phi^2}{(1-z)}+\frac{\mu^2}{z}-\frac{\phi z}{(1-z)}+\mu\right]f(z)=0$$

Finally solving and arranging to standard form as

$$\mathrm{z}(1-\mathrm{z})f''(z)+[(1+2\mu)-(2\mu+2\phi+1)z]f'(z)-[(\mu+\phi)^2+(\mu+\phi)]f(z)$$
$$+\left[\frac{-\epsilon}{z}+\epsilon-(\sigma z\ -\ \sigma\ +\beta_4 z\ -\ \beta_4)-\frac{\delta}{z}+\frac{1}{(z-1)}\{\alpha+\beta_1+\beta_2\}\right.$$
$$\left.-\beta_3(z^3-3z^2+3z-1)+\frac{\phi^2}{(1-z)}+\frac{\mu^2}{z}-\frac{\phi z}{(1-z)}+\mu\right]f(z)=0$$

Arranging two last terms like below

Used above:$\phi-\frac{\phi}{(1-z)}=\frac{\phi(1-z)-\phi}{(1-z)}=\frac{\phi-\phi z-\phi}{(1-z)}=-\frac{\phi z}{(1-z)}$

$$\mathrm{z}(1-\mathrm{z})f''(z)+[(1+2\mu)-(2\mu+2\phi+1)z]f'(z)-[(\mu+\phi)^2+(\mu+\phi)]f(z)$$
$$+\left[\left(\frac{-\epsilon+\mu^2}{z}\right)+(\sigma+\beta_4-3\beta_3)z+(\epsilon-\sigma-\beta_4-\beta_3+\delta+\phi+\mu)\right.$$
$$\left.+\left(\frac{-\alpha z^2+\phi^2-\phi+\alpha+\beta_1+\beta_2}{(1-z)}\right)-z^3\beta_3+3\beta_3 z^2\right]$$
$$=0 \qquad (23)$$

$$(\sigma + \beta_4 - 3\beta_3) = 0, =>, -\sigma = \beta_4 - 3\beta_3, -\epsilon + \mu^2 => \epsilon$$

$$= \mu^2, \mu^2 + \beta_4 - 3\beta_3 - \beta_4 - \beta_3 + \delta + \phi + \mu = 0 => \mu^2 + \delta + \phi + \mu = 0$$

$$\mu^2 - 4\beta_3 - \beta_3 + \delta + \phi + \mu = 0$$

$$\mu^2 - 4\beta_3 - \beta_3 + \delta + \phi = 0 => \phi = -(\mu^2 + \delta - 5\beta_3)$$

Again equation (20) can be written as,

$$\mathrm{z}(1-\mathrm{z})f''(z) + [(1+2\mu) - (2\mu + 2\phi + 1)z]f'(z) - \left[\left(\mu + \phi + \frac{1}{2} + \sqrt{\frac{1}{4}}\right)\left(\mu + \phi + \frac{1}{2} - \sqrt{\frac{1}{4}}\right)\right] f(z) = 0 \qquad (24)$$

$$\left(\mu + \phi + \frac{1}{2} + \sqrt{\frac{1}{4}}\right)\left(\mu + \phi + \frac{1}{2} - \sqrt{\frac{1}{4}}\right)$$

$$= \left(\mu + \phi + \tfrac{1}{2}\right)^2 - \left(\sqrt{\tfrac{1}{4}}\right)^2$$

$$= \mu^2 + \phi^2 + \tfrac{1}{4} + 2\mu\phi + \phi + \mu - \tfrac{1}{4}$$

$$= \mu^2 + \phi^2 + 2\mu\phi + \mu + \phi$$

$$= (\mu + \phi)^2 + (\mu + \phi)$$

The Hypergeometric function is defined for $|z| < 1$ by the power series

$$\square_2 F_1(\mathrm{a}, \mathrm{b};\ \mathrm{c};\ \mathrm{z}) = \sum_{n=0}^{\infty} \frac{(\mathrm{a})_n (\mathrm{b})_n}{(c)_n} \frac{z^n}{n!} = 1 + \frac{ab}{c}\frac{z}{1!} + \frac{a(a+1)b(b+1)}{c(c+1)}\frac{z^2}{2!} + \cdots$$

Here, $(a)_n = \frac{\Gamma(a+n)}{\Gamma(a)}$, $(b)_n = \frac{\Gamma(b+n)}{\Gamma(a)}$, $(c)_n = \frac{\Gamma(c+n)}{\Gamma(c)}$, Putting these in the above equation and simplifying we get,

$$F(z) = \square_2 F_1(\mathrm{a}, \mathrm{b};\ \mathrm{c};\ \mathrm{z}) = \frac{\Gamma(\mathrm{C}_1)}{\Gamma(\mathrm{a}_1)\Gamma(\mathrm{b}_1)}$$

And, the Hyper- geometric function is a solution of Euler's Hyper geometric differential equation

$$z\,(z-1)\frac{d^2\omega}{dz^2}+[c-(a+b+1))]\frac{d\omega}{dz}-ab\omega=0$$

Here, we Consider,a_1,b_1 and $c_1$are unknown parameters whose values are expressed as

$a_1=\left(\mu+\phi+\frac{1}{2}+\sqrt{\frac{1}{4}}\right)$, $b_1=\left(\mu+\phi+\frac{1}{2}-\sqrt{\frac{1}{4}}\right)$ and $c_1=1+2\mu$

Now, substituting the value of $f(z)$ with these parameter in $\psi(z)=z^{\mu}(1-z)^{\phi}f(z)$, we get

$$\psi(z)=z^{\mu}(1-z)^{\phi}2\mathrm{F1}(\mu+\phi+\frac{1}{2}+\sqrt{\frac{1}{4}},\mu+\phi+\frac{1}{2}-\sqrt{\frac{1}{4}};1+2\mu;z) \qquad (25)$$

Ifa_1,b_1, and $c_1$is equal to the negative of integer (n) then Hypergeometric function $f(Z)$ will become a polynomial with n = 0,1,2,3,...,n_{max} integer. Applying quantum condition (Okorie et al., 2018)we have,

$$\mathrm{a}_1=-\mathrm{n}$$

$$-n=\mu-\mu^2-\delta+5\beta_3+\frac{1}{2}+\sqrt{\frac{1}{4}}$$

$$\mu=-n+\mu^2+\delta-5\beta_3-\frac{1}{2}-\sqrt{\frac{1}{4}}$$

since we have $-\phi=\mu^2+\delta-5\beta_3$

$$\mu=-n+\mu^2+\delta-5\beta_3-\xi$$

Where $\frac{1}{2}+\sqrt{\frac{1}{4}}=\xi$,

$$\mu^2-\mu+\delta-5\beta_3-\xi-n=0$$

Comparing with quadratic Equation, a$x^2+bx+c=0$we, get

a=1, b= -1, c= $\delta-5\beta_3-\xi-n$

$$x = \left(\frac{-b \pm \sqrt{b^2 - 4ac}}{2a}\right)$$

$$\mu = \frac{1 \pm \sqrt{1 - 4.1.(\delta - 5\beta_3 - \xi - n).}}{2.1}$$

$$\mu = \frac{1 \pm \sqrt{1 - 4(\delta - 5\beta_3 - \xi - n)}}{2}$$

The Equation is valid only when$\left(1 - 4(\delta - 5\beta_3 - \xi - n)\right)$ is perfect square .ie. $1 - 4(\delta - 5\beta_3 - \xi - n) = \chi^2$

$$\mu = \frac{1 \pm \sqrt{\chi^2}}{2}$$

$$\mu = \frac{1 \pm \chi}{2}$$

Taking positive and negative, we get

$$\mu_+ = \frac{1+\chi}{2} \text{ and,} \mu_- = \frac{1-\chi}{2}$$

Squaring both side we get, $\mu_+^2 = \frac{1+2\chi+\chi^2}{4}$ and,$\mu_+^2 = \frac{1-2\chi+\chi^2}{4}$

Since we have $\epsilon = \mu^2$

Or,$\epsilon_+ = \frac{1+2\chi+\chi^2}{4}$and $\epsilon_- = \frac{1-2\chi+\chi^2}{4}$

Now substituting value of μ in above we get

$$\epsilon_+ = \frac{1}{4}[1 + 2\{1 - 4(\delta - 5\beta_3 - \xi - n)\} + \{1 - 4(\delta - 5\beta_3 - \xi - n)\}^2]$$

$$\epsilon_- = \frac{1}{4}[1 - 2\{1 - 4(\delta - 5\beta_3 - \xi - n)\} + \{1 - 4(\delta - 5\beta_3 - \xi - n)\}^2]$$

Substituting the value in $\frac{2mE_{nl}}{\hbar^2\eta^2} = -\epsilon \Rightarrow -\frac{2mE_{nl}}{\hbar^2\eta^2} = \epsilon$

For positive

$$-\frac{2\mathrm{mE_{nl}}}{\hbar^2\eta^2} = \frac{1}{4}[1 + 2\{1 - 4(\delta - 5\beta_3 - \xi - n)\} + \{1 - 4(\delta - 5\beta_3 - \xi - n)\}^2]$$

$$E_{nl} = -\frac{\hbar^2\eta^2}{8\mathrm{m}}[1 + 2\{1 - 4(\delta - 5\beta_3 - \xi - n)\} + \{1 - 4(\delta - 5\beta_3 - \xi - n)\}^2] \quad (26)$$

For Negative

$$-\frac{2\mathrm{mE_{nl}}}{\hbar^2\eta^2} = \frac{1}{4}[1 + 2\{1 - 4(\delta - 5\beta_3 - \xi - n)\} + \{1 - 4(\delta - 5\beta_3 - \xi - n)\}^2]$$

$$E_{nl} = -\frac{\hbar^2\eta^2}{8\mathrm{m}}[1 - 2\{1 - 4(\delta - 5\beta_3 - \xi - n)\} + \{1 - 4(\delta - 5\beta_3 - \xi - n)\}^2] \quad (27)$$

3.2 Thermodynamic Properties (Okon et al., 2022).

$$Z_{vibration} = \sum_{n=0}^{n} e^{-\beta E_{nl}}, where\ \beta = \frac{1}{k_B T} \quad (28)$$

$$Z_{vibration} = \sum_{n=0}^{n} e^{\beta\frac{\hbar^2\eta^2}{8\mathrm{m}}[1+2\{1-4(\delta-5\beta_3-\xi-n)\}+\{1-4(\delta-5\beta_3-\xi-n)\}^2]} \quad (28)$$

3.2.1 Vibrational mean energy

$$U(\beta) = \frac{\partial}{\partial\beta}(\ln Z_{vib}(\beta)) = \frac{\partial}{\partial\beta}\left(\ln\left\{e^{\beta\frac{\hbar^2\eta^2}{8\mathrm{m}}[1+2\{1-4(\delta-5\beta_3-\xi-n)\}+\{1-4(\delta-5\beta_3-\xi-n)\}^2]}\right\}\right) \quad (29)$$

$$U(\beta) = \frac{\partial}{\partial\beta}(\ln Z_{vib}(\beta)) = e^{\beta\frac{\hbar^2\eta^2}{8\mathrm{m}}[1+2\{1-4(\delta-5\beta_3-\xi-n)\}+\{1-4(\delta-5\beta_3-\xi-n)\}^2]} \quad (29)$$

3.2.2 Vibrational mean free energy

$$F(\beta) = -k_B T\ ln\big(Z_{vib}(\beta)\big) = -k_B T \ln\left\{e^{\beta\frac{\hbar^2\eta^2}{8\mathrm{m}}[1+2\{1-4(\delta-5\beta_3-\xi-n)\}+\{1-4(\delta-5\beta_3-\xi-n)\}^2]}\right\} \quad (30)$$

3.2.3 Vibrational specific heat capacity

$$C_s(\beta) = k_B\,\beta^2 \frac{\partial^2}{\partial \beta^2}(\ln Z_{vib}(\beta))$$

$$= k_B\,\beta^2 \frac{\partial^2}{\partial \beta^2} \ln\left\{e^{\beta\frac{\hbar^2\eta^2}{8m}\left[1+2\{1-4(\delta-5\beta_3-\xi-n)\}+\{1-4(\delta-5\beta_3-\xi-n)\}^2\right]}\right\} \qquad (31)$$

3.2.4 Vibrational entropy

$$S = k_B(\ln Z_{vib}(\beta)) - k_B T \frac{\partial}{\partial \beta}(\ln Z_{vib}(\beta))$$

$$= \; k_B \ln\left\{e^{\beta\frac{\hbar^2\eta^2}{8m}\left[1+2\{1-4(\delta-5\beta_3-\xi-n)\}+\{1-4(\delta-5\beta_3-\xi-n)\}^2\right]}\right\}$$

$$- k_B T \frac{\partial}{\partial \beta} \ln\left\{e^{\beta\frac{\hbar^2\eta^2}{8m}\left[1+2\{1-4(\delta-5\beta_3-\xi-n)\}+\{1-4(\delta-5\beta_3-\xi-n)\}^2\right]}\right\} \qquad (32)$$

CHAPTER 4: RESULTS AND DISCUSSION

To study the nature of eigenvalue of screening parameters is used between 0.001 to 0.5, n=0 to 2 and l=0 to 1 for H_2, Cl_2 and HCl. The Dissociation energy of H_2, Cl_2 and HCL is 4.738 eV, 2.514 eV and 4.618 eV respectively; and equilibrium bond distance is taken 0.74,1.93 and 1.27 respectively (Huber and Herzberg, 1979; Douglas and Hoy, 1975 & Hajugeorgiou, 2010).

4.1 Comparison of Screening and screening potential

The examination of Figure 1, which illustrates the repulsive potential as a function of distance at screening parameters of 0.1, yields valuable insights into the behavior of the Manning-Rosen potential concerning diatomic molecules such as H_2, Cl_2, and HCl, both in the presence and absence of screening effects. In the absence of screening, the repulsive potential (V) exhibits an increasing trend with distance, indicating heightened interaction among molecular constituents. Upon the introduction of screening effects (VS), the repulsive potential remains elevated but at reduced levels, signifying a dampening of interaction due to screening parameters. Noteworthy is the consistent higher magnitude of the repulsive potential without screening (V) compared to the screened potential (VS) for all diatomic molecules considered. This indicates that screening effects play a moderating role, diminishing the overall repulsive potential energy within the system. Exploring further at screening parameters 0.1 reveals intriguing comparative trends among diatomic molecules. The repulsive potential for H_2 (VSH2) surpasses that of Cl_2 (VSCl2) and HCl (VSHCl), even with screening effects considered, suggesting a relatively stronger repulsive potential energy for H_2 due to size and charge distribution. These observed variations underscore the nuanced interplay between screening effects and molecular interactions, providing a more comprehensive understanding of the intricate dynamics within diatomic molecules. The higher repulsive potential for H_2 hints at distinctive electronic or structural properties, warranting thorough exploration and contributing to our understanding of the role of screening parameters in shaping potential energy landscapes.

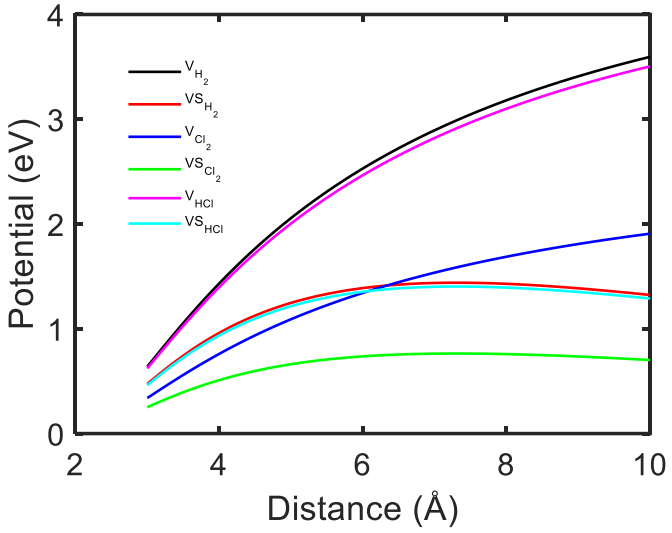

Figure 1**:** Potential with distance for screening parameters 0.1

The analysis of Figure 2, depicting repulsive potential as a function of distance at screening parameters 1, reveals distinct patterns in the behavior of diatomic molecules, including H_2, HCl, and Cl_2. As distance increases, the repulsive potential shows a consistent rise, signifying an escalating repulsion between molecular constituents under the influence of screening parameters 1. The non-screened repulsive potential is consistently greater than the screened repulsive potential, emphasizing the moderating effect of screening parameters on molecular interactions. Comparing non-screened repulsive potentials, a hierarchical order emerges, with H_2 exhibiting a higher potential than HCl, and HCl having a higher potential than Cl_2. This trend is maintained in the screened repulsive potentials, indicating that, even with screening effects considered, inherent differences in repulsive potential energies among these diatomic molecules persist. Furthermore, the comparison of repulsive potentials at screening parameters 0.1 and 1 demonstrates a decrease in repulsive potential with the lower screening parameter. The nature of repulsive potential remains similar between non-screened and screened scenarios, yet the repulsive potential is noticeably lower at screening parameter 0.1, highlighting the diminishing effect of screening as the parameter is reduced. These findings underscore the intricate relationship between screening parameters and repulsive potential energies within diatomic molecules. The consistent hierarchy in repulsive potential energies across molecules implies that molecular characteristics play a crucial role, even in the presence of screening effects. Additionally, the observed reduction in repulsive potential at screening parameter 0.1 suggests a nuanced dependence on screening parameters, offering valuable insights into the dynamic nature of molecular interactions.

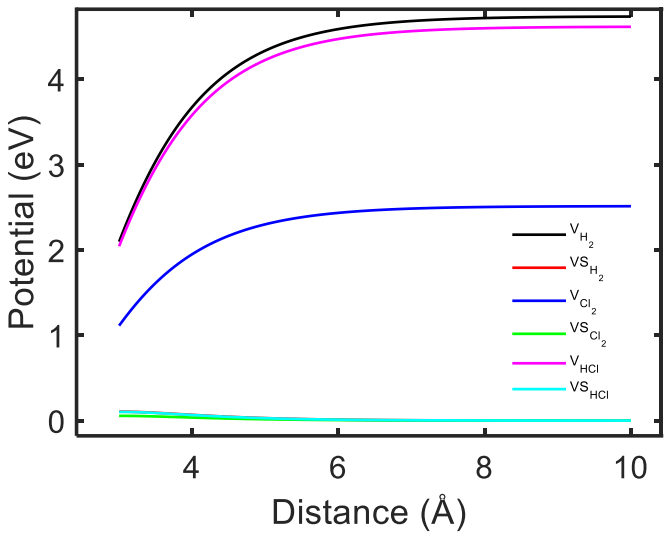

Figure 2**:** Potential with distance for screening parameters 1

Considering the information from Figure 1, illustrating the screening and non-screening Manning-Rosen potential for H_2, Cl_2, and HCl in an AB field, and the observed nature of potential increase with distance (r), parallels can be drawn with previous findings presented by Omugbe et al. in 2020 for diatomic gases (Omugbe et al., 2020). The consistent trend of potential increase with distance (r) aligns with the broader understanding of molecular interactions in AB fields, emphasizing a repulsive potential that grows as the distance between molecular constituents expands. This corroborates the general behavior observed in diatomic gases and provides additional support for the trends noted in Figure 1 (Omugbe et al., 2020). Comparing these results with the insights gained from Figures 1 and 2, a comprehensive picture emerges. In both scenarios (screening parameters 0.1 and 1), the potential energy increases with distance, showcasing the repulsive nature of interactions in AB fields. The findings not only validate the broader trends observed in diatomic gases but also highlight the nuanced influence of screening parameters on the magnitude of potential energy (Omugbe et al., 2020). The consistent hierarchy in repulsive potential energies among H_2, HCl, and Cl_2, as well as the diminishing effect of screening parameters, collectively contribute to a deeper understanding of the complex interplay between molecular characteristics and external fields. These insights, supported by both Figure 1 and previous research (Omugbe et al., 2020), contribute to the broader discourse on molecular interactions and potential energy landscapes, offering valuable implications for fields such as quantum chemistry and molecular physics.

4.2 Energy Eigenvalue of H_2, Cl_2 and HCl

The analysis of Figure 3 reveals a significant relationship between the bound electron energy and the quantum number at a certain applied field. It is observed that the bound electron energy decreases with an increase in the quantum number. Notably, the comparison between HCl, H_2, and Cl_2 electrons indicates that HCl and H_2 electrons are more tightly bound than those in Cl_2. This implies that H_2 is more stable than both HCl and Cl_2 in the given conditions. In general, the electron binding energy for Cl_2 is higher than that for HCl, and HCl's binding energy is higher than that of H_2. However, when a magnetic field is introduced, there is a notable shift in these conditions. The larger number of electrons in Cl_2 has a substantial impact on the energy eigenvalue, resulting in higher binding energy. Conversely, H_2, with a lower number of electrons, experiences a lesser effect on the energy eigenvalue, leading to an increase in its bound electron energy, making it higher than that of HCl and Cl_2. This magnetic field-induced reversal in the stability hierarchy underscores the intricate interplay between electron configurations and external magnetic fields. The findings presented in Figure 3 align with previous research (Chabi and Bounmali, 2020), confirming a similar nature of energy eigenvalues. Their results, as illustrated in Figure 3, also indicate that the energy eigenvalue at the same quantum number for H_2 is slightly higher (negative) than that for HCl. This consistency in outcomes between the current study and previous research provides robust support for the observed trends in bound electron energies. Overall, these results deepen our understanding of the nuanced factors influencing electron stability and binding energy, with implications for diverse fields, including quantum mechanics and molecular physics.

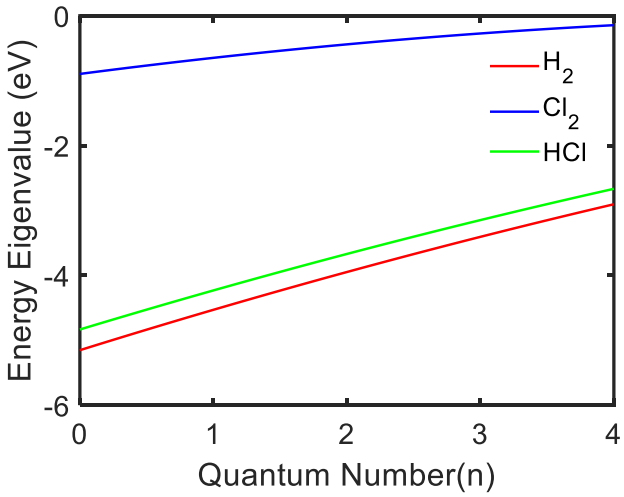

Figure 3**:** Energy eigenvalues with quantum numbers for screening parameters 0.1

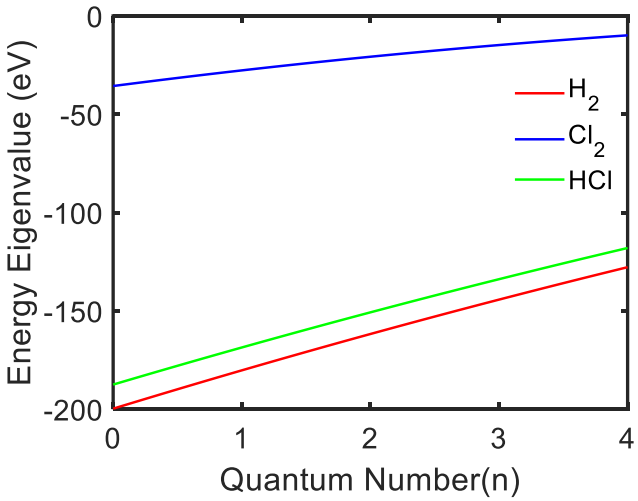

Figure 4**:** Energy eigenvalues with quantum numbers for screening parameters 0.1

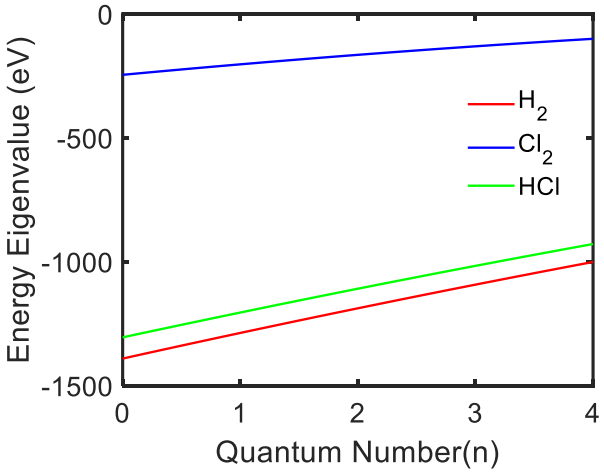

Figure 5**:** Energy eigenvalues with quantum numbers for screening parameters 1

The coherence in the energy eigenvalues concerning the quantum number, as illustrated in Figure 4, fortifies the consistency of observed trends in the present study. Noteworthy is the discernible influence of screening parameters, where a set value of 1 results in significantly higher energy eigenvalues compared to the scenario with screening parameters at 0.1. This highlights the pronounced impact of screening parameters on the stability of bonded electrons within the system. Drawing connections to the work of Ramantswana et al. in 2022, who investigated the Manning-Rosen potential in conjunction with a class of Yukawa potential, parallels emerge in the decreasing

trend of bonded electron energy with an increasing quantum number. However, a pivotal departure surfaces in the consideration of external screening parameters. In the study by Ramantswana et al., where negative values of energy eigenvalues decrease with an increasing quantum number, external screening parameters were not taken into account (Ramantswana et al., 2022). This emphasizes the unique contribution of the present research in incorporating screening parameters, unveiling their substantial influence on the behavior of bonded electrons and the associated energy eigenvalues.

This interlinking of findings accentuates the importance of screening parameters in shaping electron behavior, echoing the consistent trends observed across different potential types. The insights gained not only enhance our understanding of bonded electron dynamics but also underscore the significance of external influences, such as screening parameters, in determining the intricate interplay of quantum mechanical phenomena. This collaborative examination, building upon previous research, contributes to a more holistic comprehension of the factors governing electron stability, with broader implications for the fields of quantum mechanics and molecular physics.

Figures 6 and 7 present a comprehensive exploration of the energy eigenvalues concerning the screening parameters for atomic H_2, Cl_2, and HCl, particularly under a 20 T magnetic field. The observed trends reveal a distinct relationship between screening parameters and the bound nature of electrons. As screening parameters increase, there is a notable augmentation in the bound nature of electrons, signifying a rise in energy eigenvalues with negative values. This suggests that higher screening parameters enhance the stability of electrons, strengthening their binding within the atomic systems.

Notably, this behavior is consistent for both quantum numbers 1 and 2, indicating a uniform trend in the impact of screening parameters on electron binding irrespective of the quantum state. However, a noteworthy observation is that, for both quantum numbers, the energy eigenvalue is higher when the principal quantum number (n) is equal to 1 compared to n equal to 2. This indicates that electrons in the n=1 state experience a higher binding energy than those in the n=2 state.

This discrepancy between the energy eigenvalues for different quantum numbers can be attributed to the inherent characteristics of the quantum mechanical system. The principal quantum number

(n) signifies the energy level of an electron, with higher values corresponding to higher energy states. The observed result, where n=1 exhibits a higher energy eigenvalue than n=2, is consistent with the general quantum mechanical principle that electrons in lower energy states are more tightly bound to the nucleus. As a result, the increase in energy eigenvalues with screening parameters is more pronounced for the n=1 state, reflecting a stronger binding effect for electrons in the lower energy level.

Figures 6 and 7 underscore the pivotal role of screening parameters in influencing the bound nature of electrons within atomic systems. The consistent increase in energy eigenvalues with higher screening parameters implies an enhanced stability of electrons, and the nuanced difference between quantum states reflects the underlying principles of quantum mechanics pertaining to energy levels and electron binding. These findings contribute valuable insights into the intricate dynamics of atomic systems under the influence of magnetic fields and screening effects.

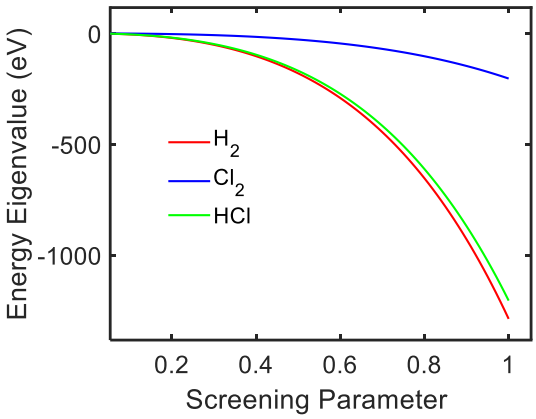

Figure 6**:** Energy eigenvalue with Screening for n=1

The current study, depicted in Figures 6 and 7, reveals a consistent trend: increasing screening parameters enhance the bound nature of electrons in atomic H_2, Cl_2, and HCl under a 20 T magnetic field. This aligns with Roshanzamir's 2023 findings for H_2 and HCl, despite their study not considering extra screening parameters (Roshanzamir's, 2023). Both investigations demonstrate that higher screening parameters result in more negative energy eigenvalues, indicating strengthened electron binding. However, the current study introduces a nuanced insight by observing a higher energy eigenvalue for n=1 compared to n=2, enriching our understanding of how different quantum states respond to screening parameters.

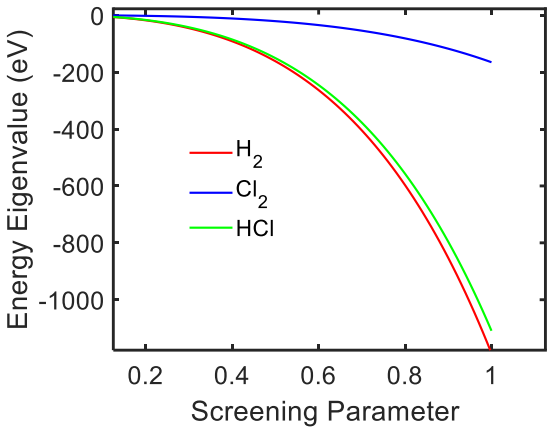

Figure 7**:** Energy eigenvalue with Screening for n=2

In Figure 8, a compelling trend is evident: a discernible decrease in energy eigenvalues with an increasing magnetic flux. This noteworthy observation implies a systematic reduction in the binding energy of electrons as the magnetic field strength intensifies. The effect is particularly pronounced in hydrogen atoms, where electrons are tightly bound, showcasing a more substantial impact of the magnetic field compared to electrons in HCl and Cl_2.

The comparative analysis further reveals significant differences in the energy eigenvalues between HCl/H_2 and Cl_2. This disparity underscores the distinct responses of different atomic systems to the influence of the magnetic field. The electrons within hydrogen atoms and HCl experience more pronounced alterations in their binding energies compared to those in Cl_2. Such variations may stem from the unique electronic configurations and structural characteristics of each atomic species.

The consistent decrease in energy eigenvalues across all considered atomic species indicates a universal trend: the magnetic field weakens the binding forces between electrons and their respective atomic nuclei. This effect can be attributed to the interaction of the magnetic field with the magnetic moments associated with the electrons, influencing their orbits and consequently altering their binding energies.

The detailed analysis of Figure 8 provides valuable insights into the intricate interplay between magnetic fields and the binding energies of electrons within different atomic systems. The observed variations among HCl, Cl_2, and hydrogen atoms underscore the importance of

considering the specific characteristics of each atomic species when evaluating the effects of magnetic fields on their electronic structures.

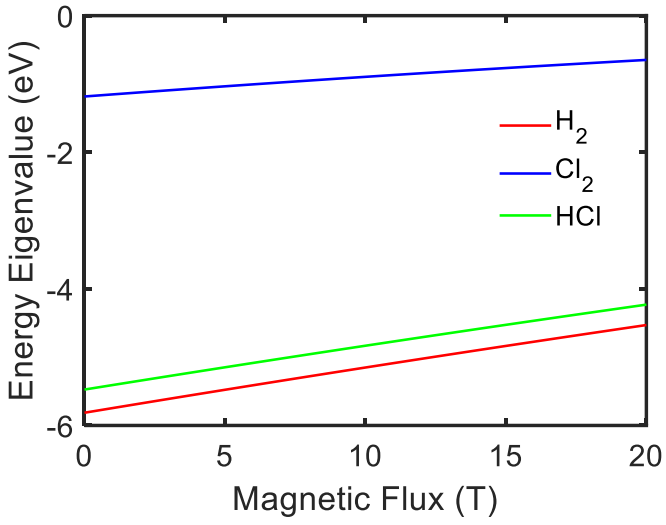

Figure 8**:** Energy eigenvalue with magnetic flux for n=1

The comparison between Figure 8 and Figure 9 reveals intriguing insights into the behavior of energy eigenvalues with varying magnetic flux for different quantum states (n=1 and n=2). Both figures exhibit a similar trend: a decrease in energy eigenvalues with an increasing magnetic flux. This consistent trend indicates that the magnetic field has a diminishing effect on the binding energy of electrons across different quantum states. However, a notable distinction emerges when comparing the two figures. In Figure 9, which represents the n=1 quantum state, the observed decrease in energy eigenvalues is less pronounced than in Figure 8. This suggests that electrons in the n=1 state experience a more substantial impact from the magnetic field, leading to a greater reduction in their binding energy. Conversely, for the n=2 quantum state, as indicated in Figure 9, the decrease in energy eigenvalues is more significant compared to the n=1 state. This implies that the magnetic field has a more pronounced effect on electrons in the higher energy level (n=2), resulting in a greater loss of binding energy. Figure 8 and Figure 9 demonstrate a general decrease in energy eigenvalues with increasing magnetic flux, the specific impact varies with quantum state. Electrons in the n=1 state experience a more significant reduction in binding energy compared to the n=2 state. This nuanced understanding highlights the quantum state-dependent effects of magnetic fields on the bound nature of electrons, providing valuable insights into the complex dynamics of atomic systems under external influences.

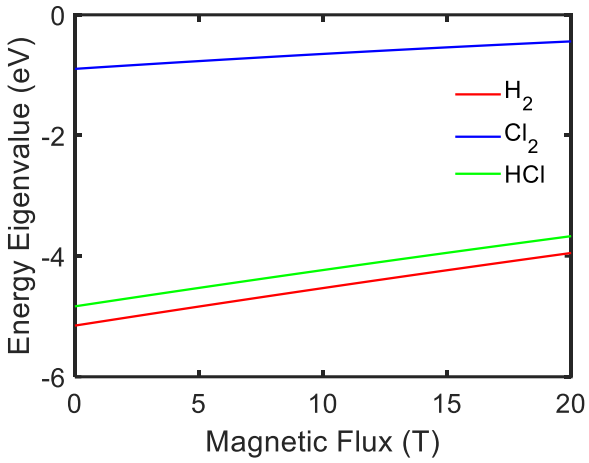

Figure 9**:** Energy eigenvalue with magnetic flux for n=2

4.3 Partition Function

The investigation of the partition function with a magnetic field in the context of the considered potential and corresponding energy eigenvalues reveals intriguing phenomena, as depicted in Figure 10. The observed trends indicate that the partition function decreases under the influence of a magnetic field. Specifically, for the n=1 quantum state and screening parameters set to 0.1, Cl_2 exhibits a lower partition function, while H_2 displays a higher partition function. This phenomenon can be linked to the interplay between the magnetic field and the energy states of electrons. The decrease in the partition function suggests a reduction in the number of accessible energy states for the electrons within the atomic systems. The magnetic field acts to quantize the energy levels, limiting the available states for electrons and thereby influencing the partition function. The disparities between Cl_2 and H_2 in terms of partition function can be attributed to their distinct electronic structures and responses to the magnetic field. H_2, with its simpler molecular structure, may experience a less disruptive impact on its electronic configuration compared to the more complex Cl_2 molecule. Consequently, H_2 exhibits a higher partition function, indicating a greater number of accessible energy states under the influence of the magnetic field. The observed decrease in partition function with a magnetic field, particularly with variations between Cl_2 and H_2, adds a layer of complexity to the understanding of how atomic systems respond to external influences. The quantization of energy levels under the magnetic field provides valuable insights into the intricate dynamics of electrons within different molecular structures, contributing to the broader understanding of quantum mechanical phenomena in the presence of external fields.

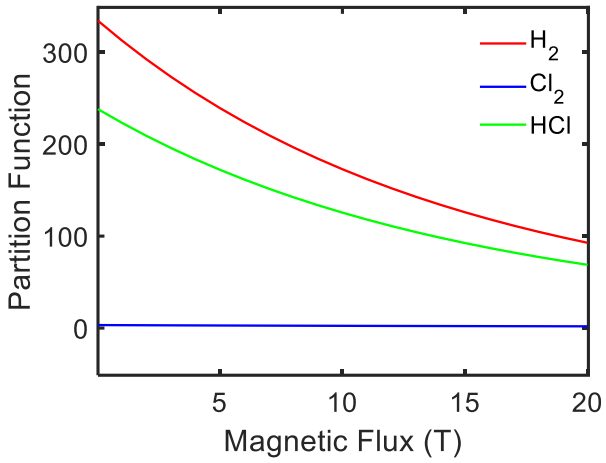

Figure 10**:** Partition function with magnetic flux for n=1 and screening 0.1

The comparison between Figure 10, which pertains to the n=1 quantum state with screening parameters set to 0.1, and Figure 11, representing the n=2 quantum state with the same screening parameters, offers a nuanced perspective on the impact of a magnetic field on the partition function. In Figure 10, for the n=1 state, it is observed that Cl_2 exhibits a lower partition function compared to H_2. This suggests that the magnetic field has a more pronounced effect on the accessibility of energy states for Cl_2 electrons in the n=1 state, leading to a reduced partition function. Conversely, H_2 displays a higher partition function, indicating a relatively lesser impact on its electronic configuration under the magnetic field.

Contrastingly, Figure 11, representing the n=2 state under the same screening parameters, reveals a different relationship. Cl_2 continues to have a lower partition function than H_2, suggesting that the magnetic field still has a more significant effect on Cl_2 electrons in the n=2 state. However, a noteworthy shift occurs when comparing the partition functions for n=1 and n=2 within each molecule. The partition function for n=1 is now higher than that for n=2, indicating that the magnetic field has a more substantial impact on the accessibility of energy states for electrons in the n=2 state. This discrepancy in the trend between n=1 and n=2 within each molecule suggests a quantum state-dependent response to the magnetic field. Electrons in different energy levels within the same atomic system may exhibit distinct sensitivities to the magnetic field, resulting in variations in the partition function.

The comparative analysis between Figures 10 and 11 underscores the complex and quantum state-dependent nature of how magnetic fields influence the partition function within atomic systems. The observed variations in partition functions for different quantum states and molecules provide valuable insights into the intricate dynamics of electrons under external magnetic fields, contributing to a deeper understanding of quantum mechanical phenomena in molecular structures.

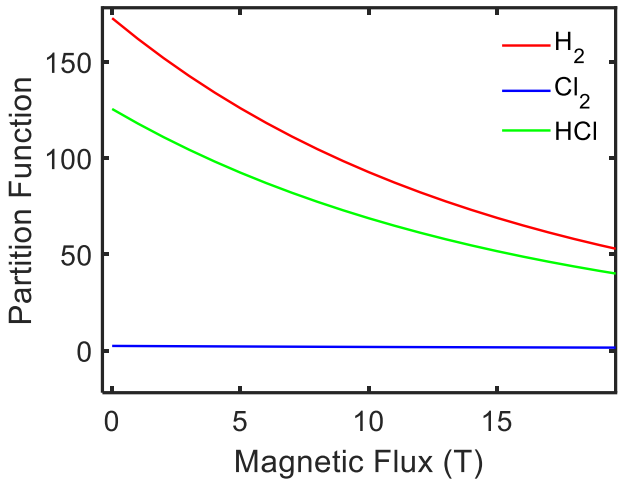

Figure 11**:** Partition function with magnetic flux for n=2 and screening 0.1

The examination of Figure 12 reveals notable insights into the behavior of the partition function with screening parameters, particularly for the n=1 quantum state. The observed trend indicates an increase in the partition function with screening parameters, suggesting that a higher screening effect leads to a greater number of accessible energy states for electrons in the n=1 state. In addition to the screening parameters, a distinctive relationship emerges when comparing the partition functions of H_2 and Cl_2. The data illustrate that, under the given conditions, the partition function of H_2 is higher than that of Cl_2 for the n=1 state. This disparity in partition functions reflects the differing electronic structures and responses of H_2 and Cl_2 to the screening parameters. The contrasting behaviors observed in partition functions under the influence of screening parameters and magnetic fields underscore the intricate interplay between these external factors and the quantum states of electrons within atomic systems. The higher partition function of H_2 compared to Cl_2 for the n=1 state suggests that, under certain conditions, H_2 may offer more diverse and accessible energy states for electrons in the given quantum state. This nuanced understanding

contributes to the broader comprehension of how atomic systems respond to external influences, shedding light on the complexities of quantum mechanical phenomena in molecular structures.

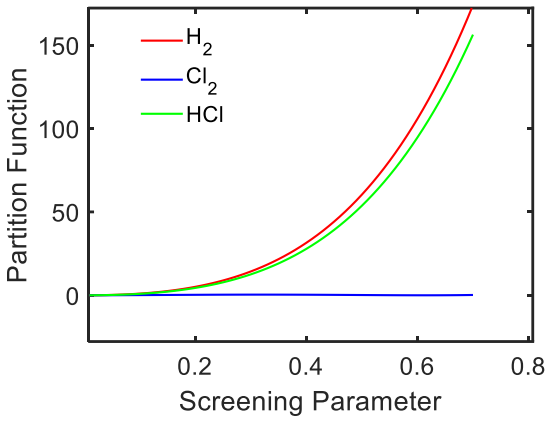

Figure 12**:** Partition function with screening parameter for n=1

The investigation presented in Figure 13 sheds light on the behavior of the partition function with screening parameters, specifically for the n=2 quantum state. The results indicate an increase in the partition function with screening parameters, highlighting that a higher screening effect results in a greater number of accessible energy states for electrons in the n=2 state. In the context of the comparison between H_2 and Cl_2, the data from Figure 13 reveal that, under the given conditions, the partition function of H_2 is higher than that of Cl_2 for the n=2 state. This difference in partition functions reflects the distinct electronic structures and responses of H_2 and Cl_2 to the screening parameters, similar to the observations made for the n=1 state in Figure 12. A noteworthy observation arises when comparing the partition functions for different quantum states within each molecule. Specifically, the partition function for n=1 is higher than that for n=2. This discrepancy underscores the quantum state-dependent response to screening parameters. Electrons in different energy levels within the same atomic system exhibit variations in their sensitivity to screening effects, resulting in differences in the number of accessible energy states. Comparing the findings from Figure 13 with those from Figure 12, a consistent trend emerges: the partition function increases with screening parameters for both n=1 and n=2 states, and H_2 consistently exhibits a higher partition function compared to Cl_2 under the same conditions. The observed quantum state dependence of the partition function further enriches our understanding of how atomic systems respond to external factors, providing valuable insights into the intricacies of electronic configurations and energy states in molecular structures.

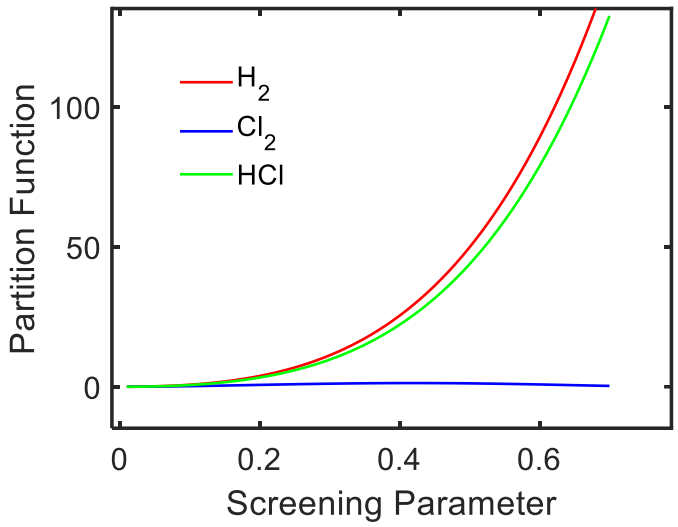

Figure 13**:** Partition function with screening parameter for n=2

CHAPTER 5: CONCLUSION

5.1 Conclusion

In conclusion, this thesis embarked on a comprehensive exploration of the nature of electron interactions within diatomic molecules, namely H_2, Cl_2, and HCl, under the influence of screening parameters, magnetic fields, and quantum states. The investigation began by scrutinizing the repulsive potential at different screening parameters, revealing intriguing trends in the behavior of the Manning-Rosen potential. The analysis demonstrated that screening effects act as moderators, diminishing the overall repulsive potential energy within the system. Notably, H_2 exhibited a consistently higher repulsive potential compared to Cl_2 and HCl, even with screening effects considered, underscoring the nuanced interplay between molecular characteristics and external influences. This is because in case of H_2 molecules the repulsion between hydrogen electron has screened electron is higher due lesser impact of nucleus as well as inside electron of hydrogen atom

Further examination of the repulsive potential at varying screening parameters unveiled a decrease in repulsive potential with lower screening values. This diminishing effect highlighted the intricate relationship between screening parameters and repulsive potential energies within diatomic molecules. The consistent hierarchy in repulsive potential energies among H_2, HCl, and Cl_2 persisted, emphasizing the influence of molecular characteristics even in the presence of screening effects. Comparisons with previous research validated the trends observed, contributing to a deeper understanding of molecular interactions and potential energy landscapes.

The study extended its focus to the energy eigenvalues, exploring their dynamics with quantum numbers, screening parameters, and magnetic fields. The findings showcased a substantial impact of screening parameters on the stability of bonded electrons, with higher screening values leading to increased energy eigenvalues. Quantum state-dependent effects were observed, with electrons in the n=1 state experiencing a more significant reduction in binding energy under a magnetic field compared to the n=2 state. This nuanced understanding aligned with previous research, emphasizing the intricate interplay between quantum states and external factors.

The examination of the partition function with magnetic fields and screening parameters added further complexity to the investigation. The decrease in partition function under a magnetic field

indicated a quantization of energy levels, limiting the accessible states for electrons. Quantum state-dependent responses were evident, with variations observed between n=1 and n=2 states within each molecule. The higher partition function of H_2 compared to Cl_2 for both quantum states suggested that H_2 may offer more diverse and accessible energy states under certain conditions.

This thesis provides a comprehensive analysis of the intricate dynamics within diatomic molecules, elucidating the roles of screening parameters, magnetic fields, and quantum states in shaping potential energy landscapes and electron behaviors. The observed trends contribute to a deeper understanding of molecular interactions, offering valuable insights for applications in quantum mechanics and molecular physics. The nuanced interplay between external influences and molecular characteristics highlighted in this study opens avenues for further research in the dynamic field of atomic and molecular physics.

5.2 Future work

Future work based on this research could involve extending the analysis to more complex molecular systems beyond diatomic molecules, exploring how different molecular configurations and larger atomic systems respond to Deng-Fan screening potentials and AB-fields. Investigating the effects of varying external magnetic fields and screening parameters on multi-electron systems could yield deeper insights into quantum state behavior and molecular stability. Additionally, the development of advanced computational models incorporating higher-order approximations and more sophisticated potential functions could enhance the accuracy of energy eigenvalue predictions. Another potential direction is to study the interplay between screening effects and other quantum phenomena, such as spin-orbit coupling, in different molecular environments. Finally, applying these findings to practical applications, such as in quantum information science or material design, could bridge the gap between theoretical predictions and experimental realizations, contributing to the broader field of quantum mechanics and condensed matter physics.

REFERENCES

Batelaan, H., & Tonomura, A. (2009). The Aharonov–Bohm effects: variations on a subtle theme. Physics Today, 62(9), 38-43. https://doi.org/10.1063/1.3226854

Douglas, A. E., & Hoy, A. R. (1975). The resonance fluorescence spectrum of C12 in the vacuum ultraviolet. Canadian Journal of Physics, 53, 1965–1975. https://doi.org/10.1139/p75-246

Dong, S. H., & Garcia-Ravelo, J. (2007). Exact solutions of the s-wave Schrödinger equation with Manning–Rosen potential. *Physica Scripta*, *75*(3), 307. **DOI** 10.1088/0031-8949/75/3/013

Chabi, K., & Bounmali, A. (2020, January/February). Thermal properties of three-dimensional Morse potential for some diatomic molecules via Euler-Maclaurin approximation. Revista Mexicana de Física, 66(1). https://doi.org/10.3136/rmex.2020.1.1.12

Edet, C. O., & Ikot, A. N. (2021). Analysis of the impact of external fields on the energy spectra and thermo-magnetic properties of N_2, I_2, CO, NO and HCl diatomic molecules. *Molecular Physics*, *119*(23), e1957170. https://doi.org/10.1080/00268976.2021.1957170

Edet, C. O., Khordad, R., Ettah, E. B., Aljunid, S. A., Endut, R., Ali, N., ... & Ikot, A. N. (2022). Magneto-transport and Thermal properties of TiH diatomic molecule under the influence of magnetic and Aharonov-Bohm (AB) fields. *Scientific Reports*, *12*(1), 15430. https://doi.org41598-022-19396-x

Falaye, B.J., Oyewumi, K.J., Ibrahim, T.T., Punyasena, M.A., & Onate, C.A. (2013). Bound state solutions of the Manning-Rosen potential. *Canadian Journal of Physics*, **91**(1), 98-104. doi:10.1139/cjp-2012-0330. https://doi.org/10.1139/cjp-2012-0330

Farout, M., Yasin, M., &Ikhdair, S.M. (2021). Approximate Bound State Solutions for Certain Molecular Potentials. *Journal of Applied Mathematics and Physics*, **9**, 736-750. doi:10.4236/jamp.2021.94052

Hassanabadi, H., Yazarloo, B. H., Ikot, A. N., Salehi, N., & Zarrinkamr, S. (2013). Exact analytical versus numerical solutions of Schrödinger equation for Hua plus modified Eckart potential. Indian journal of Physics, 87, 1219-1223. DOI: 10.1007/s12648-013-0368-3

Hajigeorgiou, P. G. (2010). An extended Lennard-Jones potential energy function for diatomic molecules: Application to ground electronic states. Journal of Molecular Spectroscopy, 263, 101–110. https://doi.org/10.1016/j.jms.2010.07.003Get rights and content

Hesam, A., Nikoofard, H., & Sargolzaei, M. (2021). Prediction of thermodynamic properties of formation of HCl at temperatures 200–1000 K. *Chemical Physics Letters*, *764*, 138276. https://doi.org/10.1016/j.cplett.2020.138276

Huber, K. P., & Herzberg, G. (1979). Molecular Spectra and Molecular Structure IV, Constants of Diatomic Molecules. Van Nostrand.

Ikhdair, S. M. (2012). Approximate l-States of the Manning-Rosen Potential by Using Nikiforov-Uvarov Method. *International Scholarly Research Notices*, *2012*(1), 201525. doi:10.5402/2012/201525

Khirali, B., Behera, A.K., Bhoi, J., &Laha, U. (2020). Scattering with Manning-Rosen potential in all partial waves. *Annals of Physics*, **412**(168044), 1-6. doi:10.1016/j.aop.2019.168044.

Karki, B., Dhobi, S. H., Nakarmi, J. J., & Yadav, K. (2022). Energy Eigenvalue and Thermodynamic Properties of q-deformed Hulthen Potential. *Bibechana*, *19*(1-2), 165-169. DOI: 10.3126/bibechana.v19i1-2.46416

Louis, H., Ita, B. I., & Nzeata, N. I. (2019). Approximate solution of the Schrödinger equation with Manning-Rosen plus Hellmann potential and its thermodynamic properties using the proper quantization rule. *The European Physical Journal Plus*, *134*(7), 315. https://link.springer.com/article/10.1140/epjp/i2019-12835-3

Oyewumi, K. J., Oluwadare, O. J., Sen, K. D., & Babalola, O. A. (2013). Bound state solutions of the Deng–Fan molecular potential with the Pekeris-type approximation using the Nikiforov–Uvarov (N–U) method. Journal of Mathematical Chemistry, 51(3), 976-991.

Falaye, B. J., Oyewumi, K. J., Ikhdair, S. M., & Hamzavi, M. (2014). Eigensolution techniques, their applications and Fisher's information entropy of the Tietz–Wei diatomic molecular model. Physica Scripta, 89(11), 115204. DOI: 10.1088/0031-8949/89/11/115204

Safronova, M. S., Budker, D., DeMille, D., Kimball, D. F. J., Derevianko, A., & Clark, C. W. (2018). Search for new physics with atoms and molecules. Reviews of Modern Physics, 90(2), 025008. DOI:https://doi.org/10.1103/RevModPhys.90.025008

Okorie, U.S., Ikot, A.N., Onyeajub, M.C., &Chukwuocha, E.O. (2018). A study of thermodynamic properties of quadratic exponential-type potential in D-dimensions. Revista Mexicana de Física, 64, 608–614. doi:10.3139/9783486796963.ch27.

Okon, I.B., Isonguyo, C.N., Onate, C.A., Antia, A.D., Purohit, K.R., Ekott, E.E., Essien, K.E., William, E.S., &Asuquo, N.E. (2022). Eigen solution and thermodynamic properties of Manning Rosen plus exponential Yukawa potential. World Journal of Applied Science and Technology, 14(2), 91–99. doi:10.4314/WOJAST.v14i2.91.

Omugbe, E., Osafile, O. E., & Okon, I. (2020, May). WKB Energy Expression for the Radial Schrödinger Equation with a Generalized Pseudoharmonic Potential. Asian Journal of Physical and Chemical Sciences, 8(2). https://doi.org/10.9734/ajopacs/2020/v8i230112

Ramantswana, M., Ikot, A. N., Rampho, G. J., Edet, C. O., & Okorie, U. S. (2022, July–December). Thermodynamic functions of Manning-Rosen plus a class of Yukawa potential using Euler-Maclaurin formula. Revista Mexicana de Física E, 19, 020204. https://doi.org/10.3136/rmex.2022.020204

Roshanzamir, M. (2023). Thermal Responses and the Energy Spectral of Diatomic Molecules Using Nikiforov–Uvarov Methodology. Mathematics, 11, 3338. https://doi.org/10.3390/math11153338

Wang, P. Q., Liu, J. Y., Zhang, L. H., Cao, S. Y., & Jia, C. S. (2012). Improved expressions for the Schiöberg potential energy models for diatomic molecules. Journal of Molecular Spectroscopy, 278, 23-26. https://doi.org/10.1016/j.jms.2012.07.001

Zhang, M. C., & An, B. (2010). Analytical solutions of the Manning-Rosen potential in the tridiagonal program. *Chinese Physics Letters*, *27*(11), 110301. DOI 10.1088/0256-307X/27/11/110301